Chapter 4 – COMPONENT MODELING FOR SYSTEM MODELS

4.1 INTRODUCTION

When a component-based engine model is used, the model capability and fidelity is generally limited by the component model characteristics available for the engine. The simulation will often be a trade-off between what is desired for system model capability and fidelity and what can be achieved with the available component models.

Component model characteristics important for consideration are:

- ***Accuracy*** – Does it match reality for overall component-performance?
- ***Detail*** – Does it provide all parts of the model at the required level? (Cooling Circuits, Seal Leakage, Purge Flows, Localized Transient Effects)
- ***Fidelity*** – Does it model all of the components at the required level of detail? (Average, Radial Profile, 3-D, Boundary Layer)
- ***Functionality*** – Does it have the required capability? (In-Stall Performance, Variable Stators and Bleed, Low Water Vapor, Vitiated Air, Rain or Ice, Clearance and Heat Transfer Effects)
- ***Complexity*** – Execution speed, data required, model expertise required, computer limitations.
- ***Range of Operation*** – Off-design, low and high speed.
- ***Compatibility with System Model and Other Component Models*** – Installation and use in system simulation, development overhead, consistency with accuracy and functionality of other models.

Components for modeling will be divided in the classical manner: gas path components such as inlet, compressor and turbine, and other components such as control systems and power train.

Table 4.1 and **Table 4.2** summarize the requirements for component models for effective use in various types of simulations. **Table 4.3** identifies component model requirements for special or secondary effects within these component models. This section contains a brief summary for each of the primary component models used in turbine engine simulations.

Table 4.1: Table of Component Model Requirements and Characteristics by Level of Fidelity

	High Fidelity	**Medium Fidelity**	**Low Fidelity**
Functionality	Limited	Limited to High	Limited to High
Complexity	High	Medium to High	Low
Range of Operation	Limited	Limited to Full Range	Limited to Full Range
Compatibility with External Models	Low	Low to High	High

Table 4.2: Table of Component Model Requirements and Characteristics by Engine Life Cycle Application

	Conceptual	Detail Design	Test and Validation	Fleet Support
Functionality	Limited	High	Limited to Medium	Limited
Complexity	Low to Medium	Medium to High	Low to High	Low
Range of Operation	Limited to Full Range	Full Range	Limited	Limited
Consistency with External Models	High	High	Low	Low

Table 4.3: Table of Secondary Effects Potentially Required by Component Models

Effects	Fan	Booster	Compressor	Turbine
Variable IGV/Stator Off-Schedule Effects	X	X	X	X
Reynolds Number Index Effects	X	X	X	X
Fan/Booster Effects due to BPR and O/L	X	X		
Distortion Effects	X	X	X	X
Blade Untwist Effects	X	X	X	
Clearance Variation Effects	X	X	X	X
Gas Property Variation Effects	X	X	X	X
Deterioration Effects	X	X	X	X
Inter-stage Bleed Effects	X	X	X	X
Heat Soak and Volume Dynamic Effects	X	X	X	X

4.2 GAS PATH COMPONENT CHARACTERISTICS REQUIRED BY ENGINE MODELS

4.2.1 General Program Requirements

The steady-state program is intended to represent the steady-state performance of the engine. Steady state means all inputs are constant and time derivatives are zero. The transient program is intended to provide simulation of engine response to input variables with an equivalent sine wave frequency content of up to 50 – 110 hertz (Hz). A minimum requirement of the transient program is the ability to adequately simulate the effects of normal throttle movements and operational dynamic events. Advanced transient models include starting as well as special events such as engine surge and instantaneous, non-commanded, load shed events.

A component-based engine description enables the user to identify the engine configuration and its general characteristics including operating and control limits that are functionally dependent on variable engine parameters. Critical to the accuracy of component-based models is the station identification. Station identification is a numbering system that is used to identify the points in the gas flow path that are significant to the propulsion system performance definition. Integers represent the interface planes between major components, such as the inlet exit and the compressor entry. When additional stations are needed within a component, decimals are used such as 2.7 for a compressor bleed extraction station. The system provides for the consistent definition of the process being undergone by the gas, regardless of the type of engine cycle. The six main processes specifically isolated are:

- Kinetic compression (inlet/diffuser);
- Mechanical compression/work addition/fluidic compression (compressor/propeller);
- Heat addition or exchange (combustor/augmentor/heat exchanger);
- Mechanical expansion/work extraction (turbine);
- Kinetic expansion (nozzle); and
- Mixing (mixer/ejector).

Figure 4.1, **Figure 4.2**, and **Figure 4.3** illustrate representative engine configurations and the associated station designations **[4.1]**.

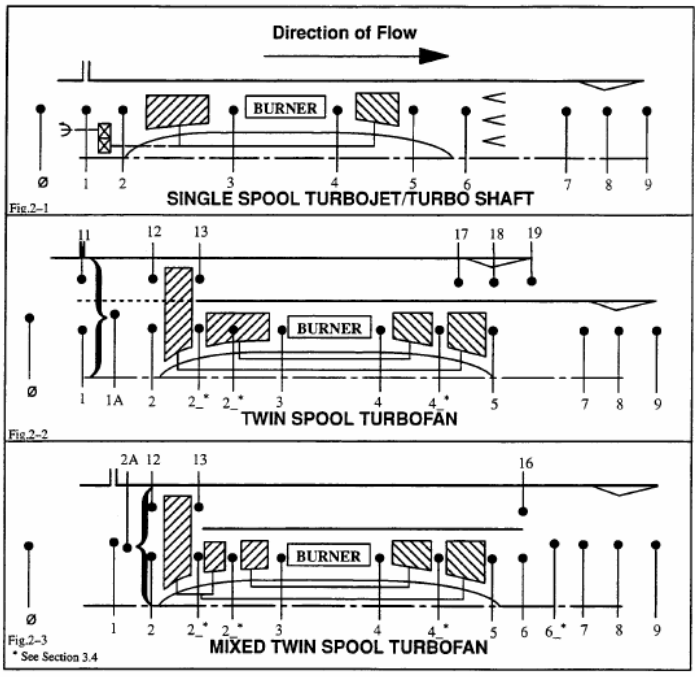

Figure 4.1: Station Designation for Single Spool Turbojet and Turboshaft and Twin Spool Turbofan.

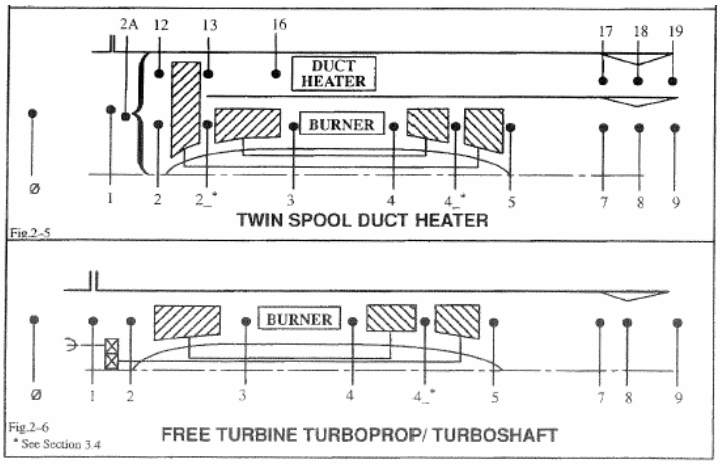

Figure 4.2: Station Designation for Twin Spool Duct Heater and Free Turbine Turboprop/Turboshaft.

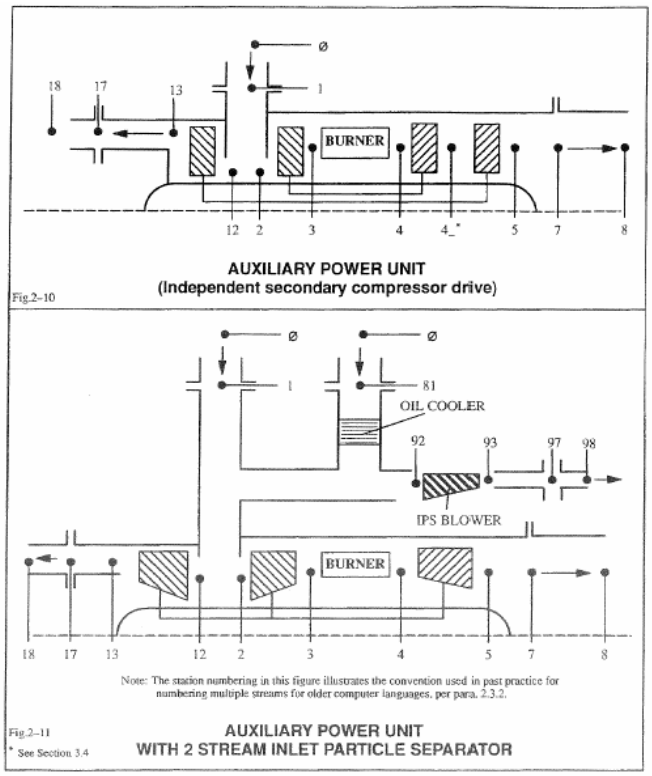

Figure 4.3: Station Designations Auxiliary Power Unit Types; Two-Spool and with Separate Stream Inlet Particle Separator.

4.2.2 Compressors

4.2.2.1 Modeling

A compressor map is the 0-D representation of its performance, showing the mass flow and efficiency of the compressor for a range of operating conditions. It may also include stall line operating limits and various flutter boundaries, as shown in **Figure 4.4**. The requirements for the map vary with their application. For engine and control system design, maps may be required to run from near zero speed to extreme over speed conditions that are beyond shaft break limits, and from stall down to windmill pressure ratios less that unity. For special studies, post-stall maps may be required.

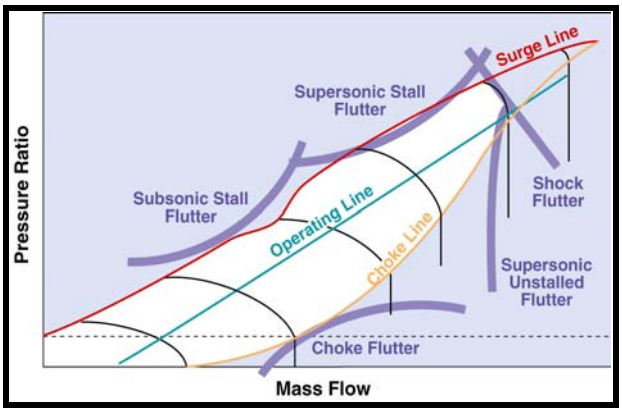

Figure 4.4: Representative Compressor-Map, with Surge-Line, Speed-Line, Efficiency Contours, and Flutter Boundary.

A map represents the performance for a nominal set of conditions that may include:

- Stator position;
- Bleed amount and location;
- Entrance temperature, pressure and gas properties (including Reynolds number, gas composition changes such as water vapor or combustion products); and
- Tip clearance.

Knowing the upstream conditions (T, P) and rotational speed, and eventually variable guide vane positions in case of a variable geometry compressor, compressor modeling predicts the outlet conditions (W, T, P) and surge margin.

4.2.2.2 Fixed Geometry Compressor

Compressor operation is characterized by the velocity triangles, on which the enthalpy rise (thus pressure ratio and efficiency) and the mass flow depend.

Dimensional analysis shows that a velocity triangle similitude must be based on a Mach number similitude.

For this reason, the classical approach to describe the compressor operation uses the two following reduced parameters:

$$W2R2 = \frac{W2\sqrt{T2}}{P2}\frac{101.325}{\sqrt{288.15}} \qquad \textbf{Eq. 4-1}$$

Inlet corrected mass flow, which depends only on axial Mach number at compressor inlet (in non-viscous flow).

$$XNR2 = \frac{XN\sqrt{288.15}}{T} \qquad \textbf{Eq. 4-2}$$

Corrected speed is proportional to the tangential velocity and approximates the blade tip Mach number.

When XNR2, W2R2 are fixed, the compressor state is determined and the pressure ratio P3Q2 and the efficiency E23 are known.

This way, two maps may characterize a fixed geometry compressor:

$$P3Q2 = F(XNR2, W2R2). \qquad \textbf{Eq. 4-3}$$

$$E23 = F(XNR2, P3Q2). \qquad \textbf{Eq. 4-4}$$

Very often, instead of using E23 as reduced parameter, the corrected enthalpy rise H3D2/T3 is employed.

An important feature of compressor modeling is the surge line, which sets an upper limit to the pressure ratio at a given corrected speed because of aerodynamic instability. This surge line can be described within the preceding maps as one of their limits. Showing the surge line separately allows secondary effects such as Reynolds number effects, distortion or production-scatter to be taken into account, without modifying the maps.

4.2.2.3 Importance of Compressor Maps in 0-D Models

The compressor map is key data in 0-D models, and one must be aware of the consequences of using insufficiently representative maps. The compressor characteristics are generally well known between 75% and 110% of the design speed. Below 75%, theoretical compressor models may lack precision. For over-speeds, compressor modeling is often limited by the inability of the partial test bench to reach these over-speeds in standard conditions, either because of insufficient driving power or mechanical risks.

Cold weather and high altitude computations often lead to operation at 125% or more of the design-reduced speed. Therefore compressor maps must be accurate in this region where efficiency is decreasing quickly. Accurate maps are also necessary at low speeds to determine the null power speed or the idle ratings; these speeds need to be accurately estimated because their influence on transient operations (acceleration times for example) and the controller design.

In a more general manner, the compressor map, like turbine maps, greatly determines the shape of the relationship between specific fuel consumption and thrust or power, and thus the range of the aircraft.

For all these reasons, the major improvements to be made to 0-D compressor models are linked to a better accounting of secondary effects.

4.2.2.4 Fan Representations

Because of the downstream splitter and booster sometimes present in high bypass turbofan engines, different model representations are often used for fans rather than trying to make a conventional compressor representation work. A separate map for the fan hub, booster and tip may be used. A common approach is to create a single model of the fan hub and booster, and a separate component model of the tip. This corresponds to the way test data is typically taken and simplifies matching test data.

4.2.2.5 Secondary and Environmental Effects

Secondary and environmental effects are those which are not addressed in the component model but which have a significant impact on the engine simulation, when the engine is not operating at the nominal condition assumed in the component model. The best way to address these effects is to include them directly in a component model. This is often impractical so that adjustments to the component model or model results are made to account for these operating condition differences. These models are generally closely tied to the basic component model in both methodologies. Usually they must follow a consistent approach, and provide the required accuracy.

4.2.2.6 Variable Geometry Compressor

In a variable geometry compressor, 1, 2 or more stator grids have variable settings. Very often, these settings depend on compressor reduced speed, and actuators commanded by the engine controller apply the setting laws.

When the variable grid number is low (1 or 2), it is possible to add 1 or 2 dimensions, corresponding to these supplementary degrees of freedom, to the maps described in **Table 4.3**.

This way, we have:

P3Q2 = F(XNR2, W2R2, CAL1, (CAL2)). **Eq. 4-5**

E23 = F(XNR2, P3Q2, CAL1, (CAL2)). **Eq. 4-6**

The setting laws CAL = F(XNR2) are then defined separately. This description is the most complete one because it allows the stator setting laws to be easily changed and optimized, without requiring a new map each time.

This first solution can be hard to apply if experimental data is lacking, or when the number of variable grids is important. In such cases, fixed geometry maps are used. Including the setting law for each stator is easier, because the data format is simpler and the data number is lower but the description is valid only for one setting law.

The more common arrangement is for all variable stators to be ganged, with changes in map performance based on a single reference stator position. There may be a series of maps for different reference stator positions relative to the nominal schedule. Alternatively, there may be a single base map for the nominal stator position and numerical corrections for other stator positions.

4.2.2.7 Basic Algorithm to Determine Outlet Conditions

At a given corrected speed, the reduced flow is limited between surge flow and blockage flow. To avoid computation problems during iterations, it is often preferred to use another parameter like W2RQPR = W2R2/P3Q2 (close to surge margin) as the input parameter, rather than W2R2.

The outlet conditions can be calculated via the following algorithm, using T2, P2, and XN1, as input data:

T2, XN1 → XNR2.

W2RQPR → P3Q2, W2R2.

P3Q2, XNR2 → E23.

P2, P3Q2 → P3.

T2, P3Q2, E23 → T3.

T2, P2, W2R2 → W2 (= W3 if no bleed).

The power absorbed by compressor can be calculated using the formula:

PW = W3H3 - W2H2.

4.2.2.8 Precautions – Map Construction Assumptions

Compressor maps are generally issued by either of two means:

- Theoretical aerodynamic models; and
- Rig testing.

In any case, the maps and surge line are often calculated as follows:

- For reference constant inlet conditions: T2 = 288.15 K, P2 = 101.325 kPa, that is to say Reynolds index equal to 1;
- With clean air inlet, that is to say, with low space-time pressure and temperature distortions;
- For given clearances: either constant for theoretical model or with a given (and identified) schedule for a partial test bench;

- In steady thermal operation; and
- For a rated and identified engine ventilation.

Many of these assumptions can be false in real engine operation and require specific corrections.

4.2.2.9 Precautions – Secondary and Environmental Effects

Reynolds Effect – It was said before that: reduced parameters for compressors find their origin on a Mach number similitude. But this similitude does not account for viscous effects. It is clear that boundary layer thickness and wakes have an effect on both flow and efficiency. To take into account this phenomenon, the Reynolds index is widely used:

$$IR = \frac{Re\ (T2,\ P2)}{Re\ (288.15\ K,\ 101.325\ kPa)} \qquad \textbf{Eq. 4-7}$$

The Reynolds index is 1 in standard conditions and decreases quickly when altitude increases. Therefore, the following correction is of major importance for altitude operation and is generally calibrated after either flight tests or altitude test bench trials.

The maps calculated for standard inlet conditions are modified as followed (EPOL denotes the compressor polytropic efficiency):

$$EPOL23\ (IR) = 1 - (1 - EPOL(IR=1))\ .\ IR^{-x}\quad 0.05 < x < 0.15 \qquad \textbf{Eq. 4-8}$$

$$W2R2\ (IR) = W2R2\ (IR=1)\ .\ \frac{EPOL23\ (IR)}{EPOL23\ (IR=1)} \qquad \textbf{Eq. 4-9}$$

P3Q2 (IR) is then calculated at a specific work, that is to say:

$$\frac{H3D2}{T2}\ (IR) = \frac{H3D2}{T2}\ (IR=1) \qquad \textbf{Eq. 4-10}$$

It is often necessary to correct the surge line also, especially in cases where the altitude domain is extended, as for turbofans.

Real Gas Effects – The real gas effects are partially taken into account because the enthalpy, specific, and entropy functions are estimated with experimental data. However, the compressor map often uses $XN/\sqrt{T2}$ and $W2\sqrt{T2}/P2$ as reduced parameters and these expressions only approximate Mach similitude. A better choice to account for the real characteristics of the gas would be $XN/(\sqrt{\gamma RT2})$ and $(W2\sqrt{T2})/P2\ \sqrt{R/\gamma}$, for example. Even with adjustment to the corrected parameters, changes in gas properties may require additional correction as described in an AGARD report [4.2].

Distortion Effects – Distortion effects are difficult to account for because their analysis requires extensive testing and aerodynamic computation. Furthermore, very complete air inlet instrumentation is needed to get all distortion characteristics. Such trials allow the establishment of tabulated rules, describing the effect of distortion on maps and surge line. Such corrections are critical in cases where high angle maneuvers may happen, as with combat aircraft and certain missiles, because the aircraft body may mask the air inlet. There may be also high distortion when the engine installation is not optimal, as for APUs.

Clearances and Ventilation Effects – The compressor performance is highly dependent on blade tip clearances, which depend on operating conditions. These effects are not accounted for with the use of

reduced parameters (aerodynamics origin), because clearances depend on the mechanical and thermal state of solid pieces. Furthermore, clearance changes correspond to a geometry modification. The main parameters influencing the clearances are compressor speed, the temperatures of the fluid in the compressor (blades and disk temperatures), out of the compressor (ambient conditions for casings temperature) and of course, the compressor ventilation. Mainly derived from thermo-mechanical computations, tabulated laws may be usefully added to correct maps and surge line.

4.2.3 Turbines

4.2.3.1 Modeling

Turbine modeling aims at determining outlet conditions, from knowledge of inlet conditions. This is the same as compressor modeling.

4.2.3.2 Fixed Geometry Turbines

From an aerodynamic point of view the turbine operation depends only on the velocity triangle. Therefore, for non-viscous flow, a good similitude is based on Mach numbers as for compressors. In fact, compressor and turbines modeling are very similar. The classical turbine description relies on the use of the following reduced parameters:

- XNR4 = XNH/√T4 reduced speed;
- P4Q45 : pressure ratio;
- WR4 : reduced mass flow; and
- E445 : efficiency.

In most operating conditions, the turbine nozzle guide vane is choked. Therefore, WR4 is constant. To avoid computational problems, XNR4 and P4Q45 are preferred as input parameters for modeling. As for compressors, two maps are used:

- WR4 = F(XNR4, P4Q45); and
- E445 = F(XNR4, P4Q45).

The reduced enthalpy rise H4D45/T4 is sometimes used instead of efficiency.

These two maps are sufficient to calculate the turbine outlet conditions. Nevertheless, generally, a third map is often used in combinations with these two maps to more accurately calculate the pressure losses in the ducts behind the turbine.

Contrarily, when compared to compressors, which mostly have axial outlet flows (both axial and centrifugal compressors), the flow at the turbine outlet presents an important swirl depending on XNR4 and P4Q45 (swirl itself is a reduced parameter because it characterizes the velocity triangle). Thus, the third map: SW45 = F(XNR4, P4Q45) is added.

4.2.3.3 Variable Geometry Turbines

This component is relatively rare because of the difficulties due to combining variable geometry and high temperatures. Nevertheless, it can be found in free turbine turboshaft engines that include a recuperator. In such a case, a free turbine with variable nozzle guide vanes permits optimization of the recuperator, by maintenance of a constant high temperature at its inlet. This applies even at part loads, and results in a very flat SFC = F(RWSD) curve.

As indicated by the former example, the NGV position typically is not governed by the turbine speed. Thus it is not possible to reduce the modeling of 2-D maps. The number of variable NGV stages is generally lower than two. This allows the method used in certain cases for compressors, by adding dimensions (corresponding to the variable settings) to be applied.

4.2.3.4 Efficiency Definitions for Un-Cooled and Cooled Turbines

In the following sections, the commonly used turbine performance bookkeeping methods are presented. The pros and cons for the different methodologies are discussed and correlations between the definitions are shown for single and multi-stage turbines with various amounts of cooling air. Furthermore it is pointed out, that simulating a cooled multi-stage turbine with an equivalent single-stage model requires the use of an equivalent Stator Outlet Temperature SOTeqv which differs from the true SOT.

It depends on the bookkeeping system used what the calculated impact on turbine performance is when the amount of cooling air changes. Without carefully adhering to a unique bookkeeping system with a clearly defined control volume the probability of misunderstandings in collaborative engine development projects is not to be underestimated.

The efficiency for any machine is a number that describes the technical quality of this machine. In case of a turbine the efficiency is the ratio of the shaft power delivered PW_{SD} and the ideal shaft power $PW_{SD,ideal}$ the turbine would deliver if there were no losses. However, this definition of efficiency is ambiguous since both terms PW_{SD} and $PW_{SD,ideal}$ can mean different things. In the shaft power delivered the disk windage and the bearing losses may be included or not, for example, and the ideal shaft power $PW_{SD,ideal}$ may account for the work potential of the cooling air by one of several alternative methods. Thus the number quoted as turbine efficiency will depend on how PW_{SD} and $PW_{SD,ideal}$ are defined.

In a collaborative engine development project the partners have to agree on a unique and unambiguous definition of turbine efficiency. One might say it is not important, which definition is used as long as it is unambiguous. However, there are some practical considerations to be taken into account when picking a definition:

- When a company has to switch over to a definition that was not used in previous projects then it can be difficult to translate the experience from the past to the design goal of the new turbine.
- It must be possible to evaluate the turbine efficiency from an engine test. This can require the installation of additional temperature or pressure probes for a specific definition.
- Similarly, if a turbine rig test is part of the engine development program, then the efficiency must be measurable in the rig. The translation of the rig-measured efficiency to an in-engine value should be as unambiguous as possible.
- Not all computer codes allow for a comprehensive accounting of turbine cooling air. A well-defined process is required to translate the calculated efficiency to the “in engine” efficiency.
- Last but not least the efficiency definition must be suitable for overall engine simulation. That means that the calculated exchange rates of turbine efficiency with overall engine parameters like thrust and specific fuel consumption must be reasonable guidelines during the engine development process.

4.2.3.4.1 Performance Models for Cooled Turbines

The efficiency of a turbine is always defined as the actual work divided by the ideal work available. However, the process of cooling a turbine greatly complicates the calculation of turbine efficiency. The problems arise when attempting to properly account for the cooling air. The work that actually is

available from the turbine is reduced compared to a turbine without cooling because all of the air does not enter the turbine at the same place and with the same available energy.

There are even more complications that arise when one is attempting to calculate blade efficiency. Blade efficiency is an attempt to isolate the efficiency of the blades from the rest of the turbine losses. This requires meticulous consideration of the air that passes over the tip of the blade, the drag of the disk, the pumping of the cooling air out to the cooling holes, the cooling air mixing losses, and the mechanical losses in the shaft.

4.2.3.4.1.1 Efficiency of an Un-Cooled Turbine

The isentropic efficiency of an un-cooled turbine is defined as

$$\eta_{is} = \frac{\Delta H}{\Delta H_{is}} = \frac{\frac{\gamma}{\gamma-1} R^*(T_1 - T_2)}{\frac{\gamma}{\gamma-1} R^* T_1 * \left[1 - \left(\frac{P_2}{P_1}\right)^{\frac{\gamma-1}{\gamma}}\right]} \qquad \textbf{Eq. 4-11}$$

In this equation the isentropic exponent of the gas γ is a mean value between the inlet and the exit of the turbine. The above assumes a steady state adiabatic process.

4.2.3.4.1.2 Stage Efficiency of a Cooled Turbine

There are two basically different methodologies for defining the efficiency of a cooled turbine: One can deal with the turbine as a sort of "black box" or go into the details of the expansion process. The first approach is discussed later, and we begin with models that describe a turbine stage by stage.

4.2.3.4.1.2.1 Single-Stage Turbine

Figure 4.5 shows a cooled single-stage turbine with a typical cooling air supply system. Compressor exit bleed is the source of the cooling air, and the control volume is identical to the turbine annulus. The power created within the control volume must be bigger than the net power available at the shaft because disk windage and accelerating the cooling air to blade velocity requires some power.

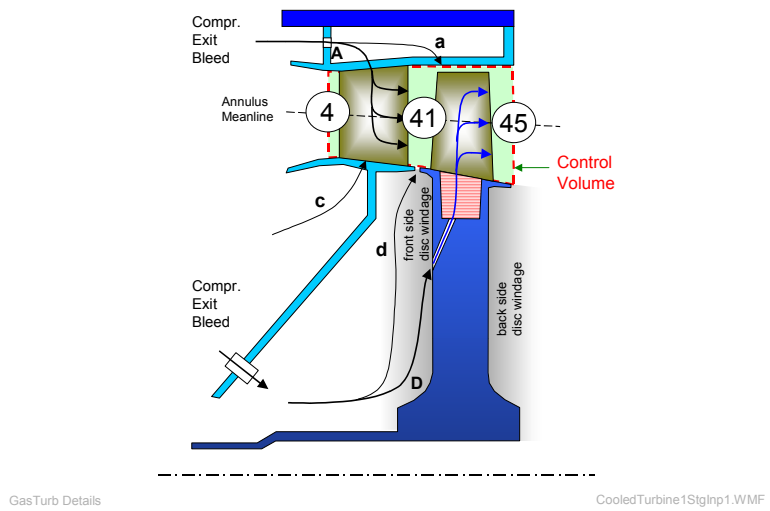

Figure 4.5: Schematic of a Single-Stage Cooled Turbine.

With the most widely used efficiency definition for each cooling air stream it is considered whether it does work in the turbine or not. However there is little consistency between companies on what flows are actually considered as part of the available work. One of the more common methods of accounting for the cooling air is to classify some air as "chargeable" and some as "non-chargeable". "Non-chargeable" air is cooling air that enters before the first rotor stage and thus is available to do work. "Chargeable" air is the cooling air that enters after the entrance to the first rotor stage and thus is considered unavailable to do work. For simplification, this air is considered as mixed with the primary flow after the rotor stage.

Usually all stator (vane) cooling air is said to do work in the rotor. Thus the rotor inlet temperature (RIT, also called stator outlet temperature SOT or T_{41}) is calculated by mixing energetically the mass flow W_4 and the stator vane cooling air W_A:

$$h(T_{41}) = \frac{W_4 * h(T_4) + W_A * h(T_3)}{W_4 + W_A} \qquad \textbf{Eq. 4-12}$$

It is assumed that the total pressure does not change while the stator cooling air is added, and thus P_{41} equals P_4, (see **Figure 4.6**). The actual expansion process begins at station 41 and yields the properties at a virtual station 415 which can only be shown in an enthalpy-entropy diagram (see **Figure 4.6**), but not in a schematic like **Figure 4.5**.

$$\eta_{stage} = \frac{PW_{SD}}{W_{41} * \Delta H_{is}}$$

PW_{SD} Shaft power delivered

ΔH_{is} Isentropic spec. work of rotor mass flow for the expansion to P_{45}

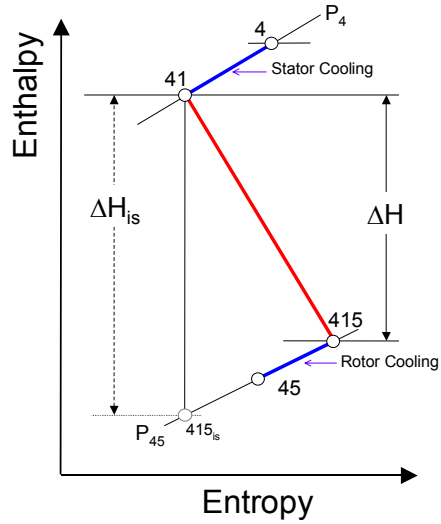

Figure 4.6: Enthalpy-Entropy Diagram for a Single-Stage Cooled Turbine.

Platform cooling air W_c and disk rim sealing air W_d normally are not considered when T_{41} is calculated since these parasitic flows do not have the potential to do work in the rotor because of lack of useful energy. Also the rotor cooling air W_D and the liner cooling air W_a cannot do any useful work in the rotor. Therefore these streams are not considered when calculating the expansion process from station 41 to the virtual station 415. They are mixed energetically together with the above mentioned parasitic flows downstream of the rotor between stations 415 and 45.

With this approach the expansion process in the rotor is the same as in an un-cooled turbine, and therefore the number used for the efficiency can be understood as that for an un-cooled turbine.

It is obvious that an adequate assignment of the work potential to the cooling air streams is important. For a turbine with given shaft power, fixed pressure ratio P_4/P_{45} and given turbine inlet temperature T_4 one

may consider a redistribution of the cooling air between stator and rotor (constant total amount of cooling air). This hypothetical redistribution has a non-trivial effect on the corresponding turbine stage efficiency as is explained in the following.

Let us assume that the sum of stator and rotor cooling air is known to be 14% of which 8% is used for stator cooling and 6% for rotor cooling. The stage efficiency is 0.9 in this example, see **Figure 4.7**. Within limits one can debate how much of the cooling air is doing work in the rotor, whether it is chargeable or not. If the amount of stator cooling air (the non-chargeable air) is decreased from 8% to 6% and simultaneously the rotor cooling air – which does no work – is increased from 6% to 8%, then the efficiency number will change. One might assume that the turbine stage efficiency number will increase from 0.9 to 0.92 because the shaft power delivered remains fixed and the ideal power is – due to the 2% rotor mass flow reduction – smaller by exactly 2%. This linear relationship is indicated by the dashed line in **Figure 4.7**.

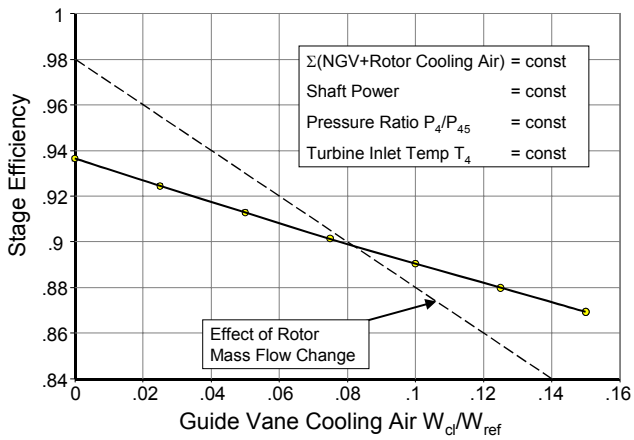

Figure 4.7: Efficiency Change for Cooling Air Re-Distribution.

However, reducing the stator cooling air increases the stator exit temperature T_{41} and this causes the efficiency to increase only about one percent as can be seen from the solid line in **Figure 4.7**. The reason for that phenomenon is the divergence of the isobar lines in the temperature-entropy diagram.

The rotor cooling air W_D must be accelerated to mean blade velocity u and that requires the specific pumping power $u^2/2$. For a proper energy balance this enthalpy change of the cooling air must be taken into account:

$$h(T_D) = h(T_3) + \frac{u^2}{2} \qquad \textbf{Eq. 4-13}$$

Often both the pumping power and the resulting increase in enthalpy of the rotor cooling air are ignored, assuming that the effects more or less cancel each other. It is not correct to account for pumping air power and at the same time to ignore the corresponding enthalpy increase of the rotor cooling air.

4.2.3.4.1.2.2 Two-Stage Turbine

Figure 4.8 shows the schematic of a two-stage cooled turbine with an associated increase in secondary air streams. Such a turbine can be modeled with two different approaches. In the first approach the two-stage turbine is simulated as an equivalent single-stage turbine. Each secondary flow is assigned a work potential. For example, the work potential of the first rotor cooling air will be approximately 50% as

opposed to the 0% for a true single-stage turbine. Consequently the calculated rotor inlet temperature will no longer be equal to the true stator exit temperature T_{41} because more than just the stator cooling air must be mixed with the main stream to get the equivalent rotor inlet temperature $T_{41eq.}$ This temperature is used to calculate the expansion process through the equivalent single-stage turbine.

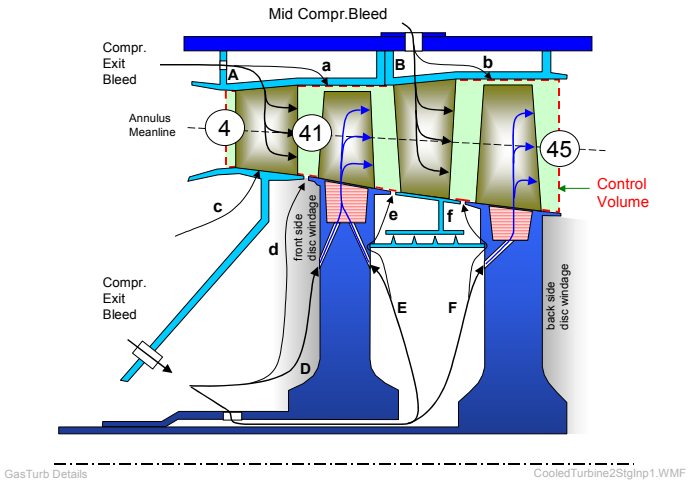

Figure 4.8: Schematic of a Two-Stage Cooled Turbine.

The calculation is basically the same as sketched in **Figure 4.6** and yields for given total turbine power and pressure ratio the equivalent stage efficiency of the turbine.

The second approach to model the two-stage cooled turbine follows the path shown in **Figure 4.9**. Each stage is modeled separately and the secondary airflows are mixed with the main stream at the appropriate stations. The cooling air of the first vane is mixed upstream of the first rotor, and the rest of the first stage secondary flows are mixed immediately downstream of the first rotor. Next the cooling air of the second vane is mixed, which yields the inlet mass flow W_{421} for the second rotor. At the exit of the second rotor the rest of the secondary airflows are mixed with the mainstream.

$$\eta = \frac{PW_{SD}}{W_{41} * \Delta H_{1is} + (W_{421} - W_{415}) * \Delta H_{2is}}$$

PW_{SD}	Shaft power delivered
ΔH_{1is}	Isentropic spec. work of rotor 1 mass flow for the expansion to P_{45}
ΔH_{2is}	Isentropic spec. work of rotor 2 mass flow added between stations 421 and 425

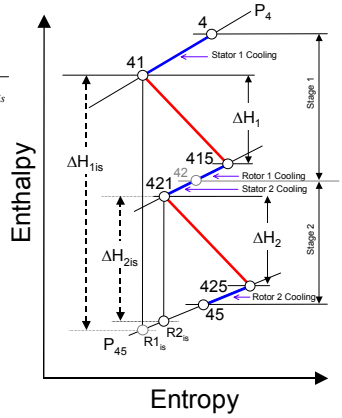

Figure 4.9: Enthalpy-Entropy Diagram for a Two-Stage Cooled Turbine.

With this approach one can study the effects of cooling air in a more direct way than with the equivalent single-stage approach. This, however, comes at a price: one needs to know the efficiency of each individual stage as well as the work distribution between the two rotors. During off-design simulations one needs two

turbine maps, one for each stage. These maps cannot be derived from engine tests because the required instrumentation is not available. Maps from a rig test are not fully representative because in such a test the cooling air effects on the flow are nearly never properly simulated because the temperature ratios between the cooling air and the main stream are not as in the engine. Moreover, the map of the second stage is affected by the variable exit swirl of the first stage and therefore theoretically several maps for selected inlet swirl angles are required.

What has been explained for the example of a two-stage turbine can easily be applied also to multi-stage turbines. The equivalent single-stage turbine is then an even more abstract model for the true process. The stage-by-stage approach is equivalent to **Figure 4.9** and results in a rather complex model.

The equivalent single-stage model gives quite different answers compared to the stage-by-stage model both with respect to the magnitude of the efficiency and – even more important – the change in efficiency when the amount of cooling air is changed. **Figure 4.10** shows how the two differently defined turbine efficiencies vary with changes in rotor 1 blade cooling and stator 2 vane cooling of a two-stage turbine. The calculation assumes again that the shaft power, the turbine inlet temperature T_4 and the pressure ratio P_4/P_{45} are given from a cycle design table, for example. Note that in addition to the blade 1 and the vane 2 cooling air streams there are a few minor parasitic air streams. These would cause a small efficiency difference in **Figure 4.10** even if no blade 1 and vane 2 cooling air is applied.

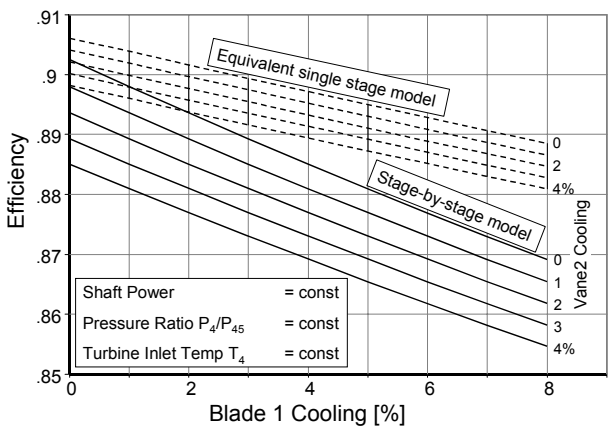

Figure 4.10: Exchange Rates of Efficiency with Cooling Air Amount.

4.2.3.4.1.3 Thermodynamic Efficiency of a Cooled Turbine

The second most used efficiency definition for a cooled turbine is called in literature the thermodynamic efficiency. In this approach the turbine is dealt with as a black box which converts thermal energy into shaft power. The input into this black box are the main stream energy flow $W_4*h(T_4)$ and many secondary air streams $W_i*h(T_i)$. All of these energy streams have the work potential which results from an isentropic expansion from their individual total pressure P_i to the turbine exit pressure P_{45}.

The thermodynamic efficiency is defined as

$$\eta_{th} = \frac{PW_{SD} + PW_{pump}}{W_4 * \Delta H_{is} + \sum W_i * \Delta H_{i,is} + \sum W_k * \Delta H_{k,pump}} \qquad \textbf{Eq. 4-14}$$

The cooled turbine process is shown in the enthalpy-entropy diagram in **Figure 4.11**. Note that within this definition no stator outlet temperature needs to be calculated. PW_{pump} is the shaft power required to

accelerate the rotor cooling air to blade velocity and $\Sigma W_k * \Delta H_{k,pump}$ is the ideal work available on these secondary streams.

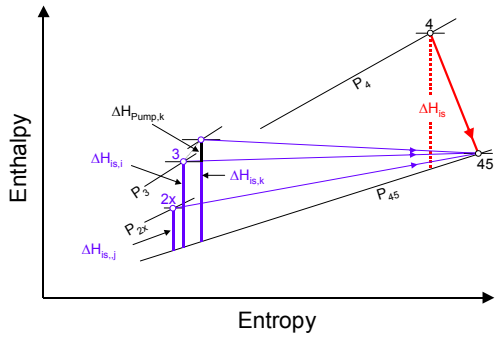

Figure 4.11: Calculation of the Thermodynamic Turbine Efficiency.

The advantage of this turbine efficiency definition is that no assumptions have to be made about the work potential of the individual secondary streams. The work potential of these streams is defined via their respective pressures and temperatures, which at least theoretically all can be measured. Thus the use of the thermodynamic turbine efficiency is less ambiguous than all the other methods mentioned above. Moreover, the thermodynamic turbine efficiency accounts for the pressure of the secondary streams while all the other definitions do not.

Figure 4.12 shows for the same turbine as used for creation of **Figure 4.10** the change in thermodynamic turbine efficiency with the amount of cooling air. In comparison to the stage-by-stage model (the dashed lines are copied from **Figure 4.10**) the effect of changing the amount of cooling air on turbine efficiency is smaller. Note that the effect of 4% vane 2 cooling air on turbine efficiency is 0.007 while the effect of 4% rotor 1 cooling air is double of that. This result is due to the difference in cooling air supply pressures and temperatures.

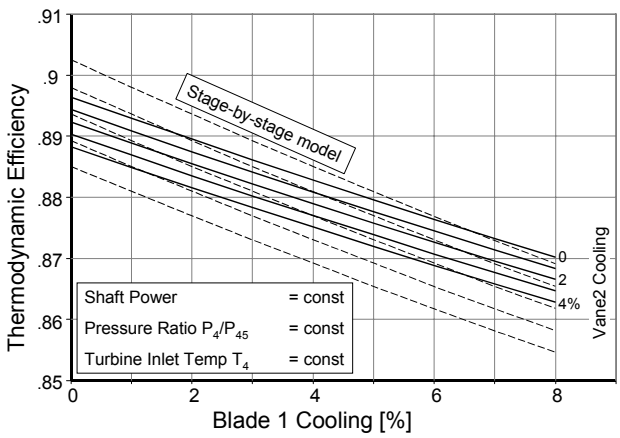

Figure 4.12: Exchange Rates of Efficiency with Cooling Air.

4.2.3.4.2 Comparison of Turbine Efficiency Numbers

In the previous sections already a few selected comparisons between the different methodologies have been shown. Here a typical example highlights how big the differences between the efficiency numbers can be, dependent on the amount of cooling air and the number of turbine stages. Since both the

distribution of the cooling air within the turbine and the work potential assigned to each secondary stream depend on the specific application the numbers quoted can only be a rough guideline for comparing turbine efficiency numbers that are based on different methodologies.

As examples serve two-stage and three-stage turbines which are designed for the same shaft power, mass flow, inlet temperature and pressure ratio. The most important data for the two turbines are shown in **Table 4.4**. The nomenclature for the secondary air streams of the two-stage turbine is that shown in **Figure 4.8**. The last stage of the three-stage turbine is assumed to be un-cooled with only a small parasitic flow at the disc 3 front rim and blade 3 shroud.

Table 4.4: Turbine Design Data

Station		**Set Conditions**			
Inlet Press P4		1144 kPa			
Inlet Temp. T4		1450 K			
Mass Flow W4		28,5 kg/s			
Shaft Power		11000 kW			
Spool Speed		14300 RPM			
Exit Press. P45		372 kPa			
Compr.Fl. W25		31,7 kg/s			
Compr.Exit P3		1180 kPa			
Compr.Exit T3		627 K			
Compr Midstage Press [kPa]		702 kPa			
Compr Midstage Temp [K]		537 K			
		2-Stage Turbine		**3-Stage Turbine**	
Cooling		% W25	%Working	% W25	%Working
NGV Cooling		5,5	100	5,5	100
Blade 1 Shroud		0,5	50	0,5	66
Vane2 Cooling		2	50	2	66
Blade 2 Shroud		0,3	0	0,3	33
NGV Platform Leak		0,4	50	0,4	66
Blade 1 Cooling (front)		5	50	5	66
Disc 1 Rim Seal (front)		0,6	50	0,6	66
Blade 1 Cooling (back)		0	50	0	66
Disc 1 Rim Seal (back)		0,2	0	0,2	33
Blade 2 Cooling		2	0	2	0
Disc 2 Rim Seal (front)		0,25	0	0,25	33
Disc 2 Rim Seal (back)				0,2	33
Disc 3 Rim Seal (front)				0,1	0
Blade 3 Shroud				0,1	0
Total	**Average**	16,75	58,2	17,15	66,6
Thermodynamic Efficiency		0,8757		0,8744	
Equivalent Single-stage Efficiency		0,8911		0,8841	
Stage-by-Stage Efficiency		0,8730		0,8540	
Single-stage Efficiency		0,9106		0,9106	

4.2.3.4.2.1 Correlations between Efficiency Definitions

In **Figure 4.13** efficiency differences are presented as a function of the cooling air amount. Note that all individual secondary air mass flows are proportional to the NGV respectively vane 1 cooling air percentage that is used as x-axis in the figure. The data corresponding to **Table 4.4** can be read from **Figure 4.13** at the x-value of 5.5%, for example.

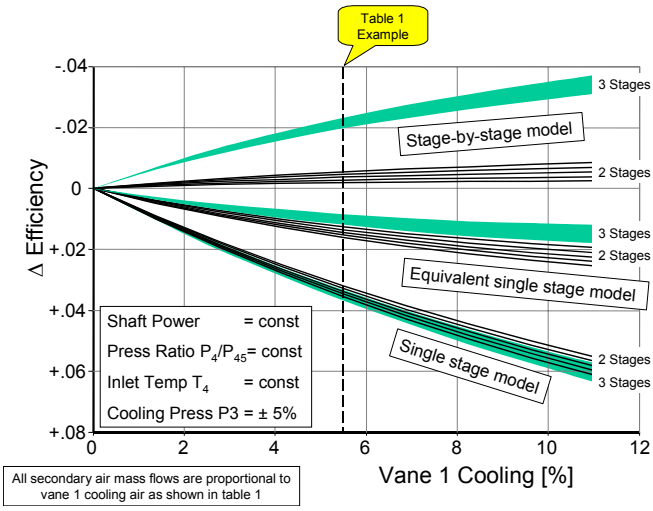

Figure 4.13: Differences between the Efficiency Numbers for Different Methodologies.

As a baseline the thermodynamic turbine efficiency described in ***Section 1.3*** is employed. The band shown about each calculation represents the sensitivity for a ± 5% variation in cooling air pressures which only has an impact on the thermodynamic efficiency calculation.

With the single-stage model all cooling air except of the first vane cooling air is assumed to do no work and it is mixed downstream of the rotor. Therefore the rotor mass flow is lower than that through the rotor of the equivalent single-stage model, because in this case part of the cooling air is assumed to do work. Since the shaft power delivered is the same, the single-stage efficiency is higher than the equivalent single-stage efficiency.

Note that the number of stages has only a minor effect on the efficiency difference for the single-stage methodologies, but a significant impact on the numbers consistent with the stage-by-stage model.

4.2.3.4.2.2 Difference between True and Equivalent T41 (Multi-Stage Turbines)

The true stator exit temperature T_{41} is calculated by energetically mixing the NGV (vane 1) cooling air $W_{cl,NGV}$ with the turbine entry mass flow W_4:

$$h(T_{41}) = \frac{W_4 * h(T_4) + W_{cl,NGV} * h(T_{cl,NGV})}{W_4 + W_{cl,NGV}} \qquad \textbf{Eq. 4-15}$$

As mentioned above, this temperature is used as rotor inlet temperature with the single-stage model. With the equivalent single-stage model more than just the NGV cooling air is mixed upstream of the first rotor, and therefore the calculated stator exit temperature T_{41eq} is significantly lower than the true T_{41}.

Also for the thermodynamic efficiency definition an equivalent turbine entry temperature is often calculated. This temperature is used for calculating the parameters in a turbine map like corrected spool

speed and corrected specific work. The numbers shown in **Figure 4.14** have been calculated by mixing energetically half of the secondary air with the turbine entry mass flow W_4.

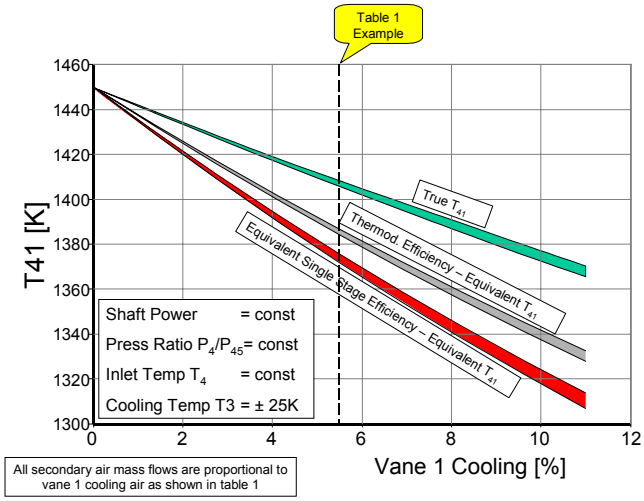

Figure 4.14: True and Equivalent Stator Exit Temperatures.

It has been explained above that the efficiency numbers quoted for the single-stage models depend on the amount of cooling air and thus the stator exit temperature T_{41}. By adjusting the NGV cooling air mass flow one can produce any number for the turbine efficiency. Thus it is also possible adjusting the NGV cooling air in such a way that the efficiency number consistent with the single-stage model is equal to the number of the thermodynamic turbine efficiency, for example.

4.2.3.4.3 Impact of the Choice of Efficiency Definition on the Results of Cycle Calculations

After having seen the differences between the various efficiency definitions it is not astonishing, that these have an important effect on the results of engine cycle calculations. **Figure 4.15** shows two carpets that were created for a high-bypass turbofan at cruise conditions with the cycle code GasTurb **[4.3]**. One carpet is valid for constant thermodynamic turbine efficiency, and the other for constant single-stage efficiency. Efficiencies were adjusted so that the top right corner points (T_4 = 1700 K, P_3/P_{25} = 12) agree. Because of the different mathematical definitions, the carpet plots diverge as one moves away from this set point of equality.

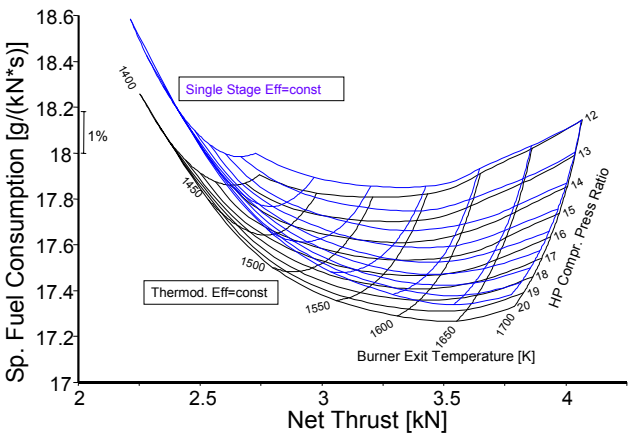

Figure 4.15: Cycle Parameter Studies with Differently Defined Turbine Efficiencies Held Constant.

In summary, this discussion of turbine efficiency definitions highlights the importance of choosing the definition that will be used in tracking the performance of the overall engine and at the same time defining the true technical quality of the turbine itself. The performance and turbine aero-engineer need to agree on what to choose for their application and what instrumentation is practicable and needed to verify the level of turbine efficiency attained.

As an evaluator it is also important to understand the impact of knowing what definition has been used in quoting the technical quality of the turbine, so that equal comparisons can be made from one turbine manufacturer to another.

4.2.3.5 Total-to-Static Turbine Maps

Generally component maps are given for total parameters, which avoid having to know the sections at inlet and outlet. Let us consider the example of a free turbine turboshaft engine.

A diverging nozzle, for slowing down the exhaust gases, follows the power turbine. The power created by the free turbine results from both total-to-total efficiency and pressure losses in the nozzle. Very often, it is difficult to evaluate the losses in the nozzle due to swirl, and the presence of struts, thus the total to total pressure ratio of the turbine is not accurately known.

To avoid this conflict between power turbine and downstream losses, a map modeling both turbine and nozzle, which uses a total to static pressure ratio P45Q59 = P45/PS9, is often used. This ratio is known more easily because PS9 is equal to the ambient static pressure. In such cases, the swirl map is not given because the nozzle losses are already included in the efficiency E4559.

This total to static map is thus given in the following form at:

- WR45 = F(XNR45, P45Q59); and
- E4559 = F(XNR45, P45Q59).

The associated drawback is that any change in nozzle geometry requires new total to static maps.

4.2.3.6 Basic Algorithm to Determine Outlet Conditions

The turbine outlet conditions can be calculated by the following algorithm using T4, P4, XN, P4Q45 as input data:

- T4, P4, WR4 → W4 = W45.
- T4, P4Q45, E445 → T45.
- P4, P4Q45 → P45.

The power created by the turbine can be calculated by: PW = W4H4 - W45H45.

4.2.3.7 Precautions – Limitations

Most remarks made for compressor maps, can be applied to turbine maps. Like compressor maps, turbine maps are issued with reference inlet conditions and a reference environment expressed as clearances, ventilation. The translation of these performances to the actual engine environment is a critical problem for 0-D models, which minimize the geometry description. This translation is even more difficult for turbines than for compressors because:

The design point for a turbine is at high temperature and pressure while turbine maps are often measured at partial test bench using cold and low-pressure air. Consequently, the corrections due to inlet conditions are much bigger than for compressors.

The temperature inlet condition for a turbine varies through a much wider range than for compressors because there is a combination of both ambient temperature range, due to the flight domain, and the power or thrust level range. Thus, the corrections are not only bigger than for compressors, but they have higher amplitudes within the operating envelope.

Nevertheless, there is one feature of turbines that in certain cases can ease their modeling. When a turbine stage is located between two choked fixed sections (either nozzle guide vane or exhaust nozzle), it is easy to prove, thanks to the critical mass flow formula, that the pressure ratio of the stage is fixed and does not depend on the operating conditions. Therefore the specific work H4D45/T4 is also constant.

Generally, the turbine drives a compressor for which $(H3-H2)/XN^2$ is quite constant (velocity triangle), so $XN/\sqrt{T4}$ is nearly constant. That means that such a turbine has a single aerodynamic operating point because both XNR4 and P4Q45 are constant. In reality, this operating point moves a bit inside the maps because of the real gas effects and the wide temperature range. Thus, HP turbine modeling is much more of an environmental modeling problem rather than an aerodynamic one. Of course, turbines such as free turbines in turboshaft engines cumulate all difficulties because their exhaust nozzle is not choked.

Most corrections mentioned for compressors, such as Reynolds effect, clearances and ventilation corrections, can be applied to turbines. The last of these has a major impact on efficiency, because cooling flows generate local distortion and aerodynamic disturbances.

Concerning the effect of distortion mentioned for compressors, the problem is slightly different for turbines because it is not due to installation or flight conditions. Here it is due to engine design, at the combustor outlet, where there is a non-uniform temperature profile. This is because of:

- Cooling of static parts in the combustor;
- Optimization to increase turbine blade creep life;
- The presence of discrete injectors and their azimuth profile; and
- Staged combustion.

It is very difficult to account for that distortion due to lack of experiments and the severity of the environment. As with compressors, more accurate reduced parameters may be used for Mach number similitude by accounting for γ and R variations:

- $XN/\sqrt{\gamma RT4}$ instead of $XN/\sqrt{T4}$; and
- $W4\sqrt{T4}/P4\ \sqrt{R/\gamma}$ instead of $W4\sqrt{T4}/P4$.

4.2.3.8 Importance of Turbine Maps in 0-D Models

As said before, what we may call a *HP turbine* has a fixed operating point. The operating point of a power turbine in a turboshaft engine, for example, is variable because the pressure ratio is not fixed. For that reason, turbine maps won't have the same criticality.

Fixed Operating Point Turbines – From the point of view of the customer, who considers the engine with a given turbine's matching, the HP turbine map is not as important as the environment and secondary effects. This is because the operating point is nearly constant. However, for the engine designer, it is important to have a good prediction of reduced speed and pressure ratio effects, in order to optimize the

initial matching, or to study eventual engine re-matching by NGV section changes, or simply to evaluate the production scatter effect.

Variable Operating Point Turbines – This case may be encountered in two configurations:

- There is one critical section behind the turbine but this section varies according to operating conditions. This is the case for an LP turbine in a military turbofan with a variable exhaust nozzle.
- There is no critical section behind the turbine. This is the case for a power turbine in a turboshaft engine.

In both cases of variable operating point turbines, the operating point may vary across a wide range within the maps and such maps will become, like compressor maps, key features of the 0-D models.

4.2.4 Burners and Augmentors

The heat addition component models typically include the primary combustor between the compressor and turbine components, and the augmentor or afterburner downstream of the turbomachinery. The component models typically differ according to the design intent and relevant operating range.

Main burners are designed for high efficiency, long life, low-pressure drop and flat temperature profiles to accommodate the downstream turbine. They must operate reliably over the aircraft envelop and all power settings.

Synonymously with *Afterburner*, the terms *Augmentor* and *Reheat* are used to describe an auxiliary burner downstream of the turbines in which the gas is reheated to provide extra thrust. These are used for limited periods, only at high power and for limited duration. Although there are many common issues, individual designs of main burner and augmentor have significant differences. A key difference between main burners and augmentors is the large variation in momentum pressure drop in the augmentor with operating condition, compared to the relatively fixed pressure drop in the main burner.

4.2.4.1 Burners

At the 0-D level, combustor representations generally model the energy rise and pressure drop across the burner, based on operating conditions and any special operating modes (number of fuel nozzles fired, number of flame-holder rings, etc.). Models may also include kinetics models for emission calculations. More detailed models may include detailed information on the temperature and pressure fields, the dilution air mixing and the fuel injection and dispersion processes.

4.2.4.2 Modeling

Modeling of combustors is relatively easier than modeling of rotating components, at least for 0-D models of classical burners, because the burning efficiency is close to 1 in many conditions. This is because they do not have any pollutant-emission constraints or non-afterburning chambers.

The combustor is considered as a black box that receives:

- Hot compressed air from an HP compressor characterized by W3, T3, P3 and eventually a non null water-air ratio WAR3; and
- Fuel characterized by its mass flow WF and its lower heating value FHV. This mass flow may be split in the case of a staged combustor.

The combustion is usually modeled as a heat addition at quasi-constant pressure (there are pressure losses). The real added heat depends on the burning efficiency of the combustor defined as:

$$EFB = \frac{W4H4 - W3H3}{WF \cdot FHV}$$ **Eq. 4-16**

This is the ratio of real heat over theoretical heat due to a perfect combustion. For classical combustors, EFB is close to 0.995 because the combustor is designed to have a quasi-stoichiometric primary zone, which guarantees both high efficiencies and stability.

In the case of low-emissions chambers required by new legislation for land based turbines, new concepts are being experimented with. Examples are LPP (Low Premixed Pre-vaporized) and RQL (Rich Quench Lean) where the primary zone is either poor or rich. This leads to lower burning efficiencies although still generally higher than 0.97.

To model the changes of burning efficiencies according to the chamber inlet conditions, the aerodynamic load Ω of the chamber is often used:

$$\Omega = \frac{W3}{P3^{1.8}\, e^{T3/300}\, VOL},$$ **Eq. 4-17**

where VOL denotes the volume of the chamber.

This parameter represents EFB as a decreasing function of Ω:

$EFB = EFB\,0 - \alpha\, \Omega^{\beta}$, with $\alpha \approx 10^{-3}$ and $\beta \approx 1.4$.

α and β coefficients depend on the combustion chamber configuration.

This equation is valid for high-pressure combustion that is reaction rate limited. At lower pressures, typically below 2 atmospheres, combustion may be flame speed limited. Although this basic relation may still be useful at low pressures, the exponents in the relationship will change dramatically. In flame spreading limited regimes, the transition from laminar to turbulent burning will also affect the correlation. This relation also assumes adequate atomization of the fuel flow. At the extreme range of fuel flow for a particular burner design, the combustion efficiency may be atomization limited. This can occur at high altitudes with low fuel flow rates when the fuel delivery mechanisms has been sized and optimized for high fuel flow levels at sea level operation.

An important feature of combustion chambers is their extinguishing limit. Below a certain fuel air ratio, the flame may be blown out leading to an engine stop. This limit has to be included in any performance simulation and especially for transient simulation.

As mentioned before, the combustion is quasi isobar; the pressure losses at the design point vary typically from 3% to 10% in certain cases, where integration constraints led to a reduction in the chamber volume (for example missile engines which have to conform to an external diameter).

The diffuser, liner cooling and fundamental heat release process result in some pressure loss that can be modeled as:

$$\frac{P4D3}{P3} = CD \times \left(\frac{W3\sqrt{T3}}{P3}\right)^2 + K*(T4/TT3 - 1)$$ **Eq. 4-18**

4.2.4.3 Basic Algorithm to Determine Outlet Conditions

The input data are: T3, P3, W3, and WF, and the chamber outlet conditions can be computed as follows:

W3, WF $\xrightarrow{\text{Mass flow conservation}}$ W4 = W3 + WF

4.2.4.4 Afterburner (Reheat) Simulation

With an afterburner the maximum thrust of a turbofan may be increased by 50 to 100% for short periods of time.

An afterburner is a fairly simple device, and it consists of only a few basic parts: a diffuser section, fuel injectors and flame-holders, a mixer, the jet pipe with a liner which controls the cooling air distribution and the nozzle.

In the diffuser section, the turbine exit guide vanes eliminate residual swirl downstream of the low-pressure turbine rotor. In the actual diffuser the Mach number is reduced from approximately 0.4 to 0.2. In this region the fuel injectors are placed in such a way that the fuel can be distributed as required.

The flame-holders stabilize the flame in the relatively high velocity environment, and the jet pipe serves as a combustion chamber, which provides time for the chemical reaction. A screech damper is necessary to suppress high-energy destructive acoustic frequencies. The screech damper is part of the liner that protects the case from high temperatures. Downstream of the afterburner a variable area nozzle is required to control the operating conditions of the turbomachinery.

The flow phenomena in a burning afterburner are extremely complex, and it is not feasible to simulate them on a purely theoretical basis with sufficient accuracy. Developing an afterburner is still an empirical task that includes the old-fashioned cut-and-try approach. An accurate simulation of the performance of an afterburner will always include some empirical correlations that are derived from engine test analysis.

An afterburner must operate over a wide range of conditions. To obtain the maximum thrust the fuel must be injected in such a way, that all of the available oxygen in the main stream is burnt. That means that the fuel-air-ratio must be very uniform at the nozzle inlet. When the fuel is not distributed evenly then there are some regions that lack fuel and others with an over-stoichiometric fuel-air-ratio. In both regions the heat release is less than maximal.

At minimum afterburner rating the fuel must be distributed stoichiometrically in the now small combustion region to prevent the flame from being blown out. In other words, the fuel must now be distributed very unevenly throughout the afterburner.

Simulation of the afterburner requires models for:

- Pressure losses in dry and reheated operation;
- Heat release of a given amount of fuel;
- Combined effect of the burning process;
- Nozzle position on the operation conditions of the turbomachinery; and
- Power requirement of the afterburner fuel pump.

For a high fidelity transient afterburner simulation the ignition process and the time needed to fill the fuel injectors that are empty during dry operation to avoid fuel coking, must also be modeled.

The following paragraphs deal mainly with the simulation of steady state afterburner operation in mixed flow turbofans. Most of the methods described are also applicable to the afterburners of straight turbojets. Practical afterburner simulation models are all of the semi-empirical type.

4.2.4.5 Dry (Non-Burning) Operation

When no fuel is injected, the afterburner behaves as a mixer, and the calculation procedures described in ***Chapter 4.2.7.2*** apply. However, the pressure losses are significantly higher than in an engine without reheat because the geometry of an afterburner must be optimized for best burning stability and efficiency, and not for minimum pressure losses.

4.2.4.5.1 Turbine Exhaust Guide Vanes

The pressure losses of the exit guide vanes depend on the swirl downstream of the low-pressure turbine rotor and the Mach number. This can be modeled with a loss characteristic that employs these parameters.

Alternatively, the exhaust guide vanes can be regarded as a part of the low-pressure turbine. The efficiency, as read from the turbine map, would then include the losses of the exhaust guide vanes.

4.2.4.5.2 Diffuser, Spray Bars and Flame-Holders

Flame holding and propagation requires a flame-holder system that creates a low velocity re-circulating air region. Such a system produces, as a by-product, significant pressure losses. Additional losses are created by the fuel injectors (spray rings or spray bars) placed upstream of the flame-holders, and the diffuser. All these losses are often lumped together and modeled as one. Since in this part of an engine the flow Mach number is subsonic under all conditions, the pressure losses of the core stream will vary proportionally to the turbine exit corrected flow squared.

Modeling the pressure losses of the bypass flow can be more difficult, especially in engines with a low bypass ratio. In this case, a significant part of the flow will pass behind the liner and only the remainder enters the afterburner at the bypass exit. Eventually the pressure downstream of the bypass flame-holders can be derived from the bypass exit pressure only with the help of an empirical correlation.

While all turbofans in series production employ afterburners with flame-holders, it should also be mentioned that there are alternatives. Mixing and burning in two-stream systems can be enhanced by swirl, and no flame-holders are then required. Turbofan swirl augmentors are described in some detail in the paper by Egan (1978) **[4.4]**.

4.2.4.5.3 Mixing

The simulation of the mixing of two streams in a constant area duct is described in ***Section 4.2.7.2***. From this calculation one gets the ideal nozzle inlet conditions when the afterburner is not lit. In practical afterburners the core and the bypass streams will not be fully mixed at the inlet of the nozzle. Total pressure and temperature will not be constant over the radius and this causes a thrust loss relative to the ideal case.

This thrust loss can be modeled with the help of the mixing efficiency defined in ***Chapter 5***. Alternatively one can use the thrust of a nozzle with fully mixed flow as a reference, and apply a thrust coefficient that brings the calculated result in line with reality.

4.2.4.5.4 Jet Pipe

The losses due to wall friction in the jet pipe are small compared to the losses caused by the flame-holders. Mixing the liner cooling air with the main stream causes another pressure loss in the jet pipe. Mostly these

two losses are not accounted for separately, and they are combined with the bypass flame-holder loss characteristic.

4.2.4.5.5 Flow Distribution and Turbomachinery Matching

In a high bypass engine without an afterburner the full bypass flow joins the core flow at the edge of the mixer. When the mixer is of the confluent type, then both streams are flowing essentially in parallel, and the static pressures of both streams are equal.

The shape of a forced mixer is quite complex, and so is the flow-field in the region where the two streams join. However, for the purpose of simulating the turbomachinery-matching of such an engine, it is sufficient to calculate the mean static pressures from the invariable effective flow areas, and request that these mean pressures are equal.

In the cycle model of a turbofan the operating points of the compressors and turbines are found with an iterative algorithm. In the first pass of an iteration through the mathematical model the operating points are only estimated values, and consequently some conditions (flow continuity and energy balance, for example) are not fulfilled. In particular, the mixer inlet conditions will be such that the static pressures of the core and the bypass stream at the mixer edge are not equal, and this results in the so-called ***mixing error***.

In turbofans with afterburner, **Figure 4.16**, a significant amount of the bypass air passes behind the liner and joins the main stream successively through the screech damper and the liner cooling air holes. The nozzle cooling air does not enter the afterburner at all. Thus, only a part of the bypass air enters the mixer. Moreover, at the entry to the mixer the geometry is often very complex. The flame-holders create re-circulation zones of significant size just within the region where the simple mixer model assumes static pressure balance. The question arises, what are the effective mixer areas, and are they invariable for all operating conditions?

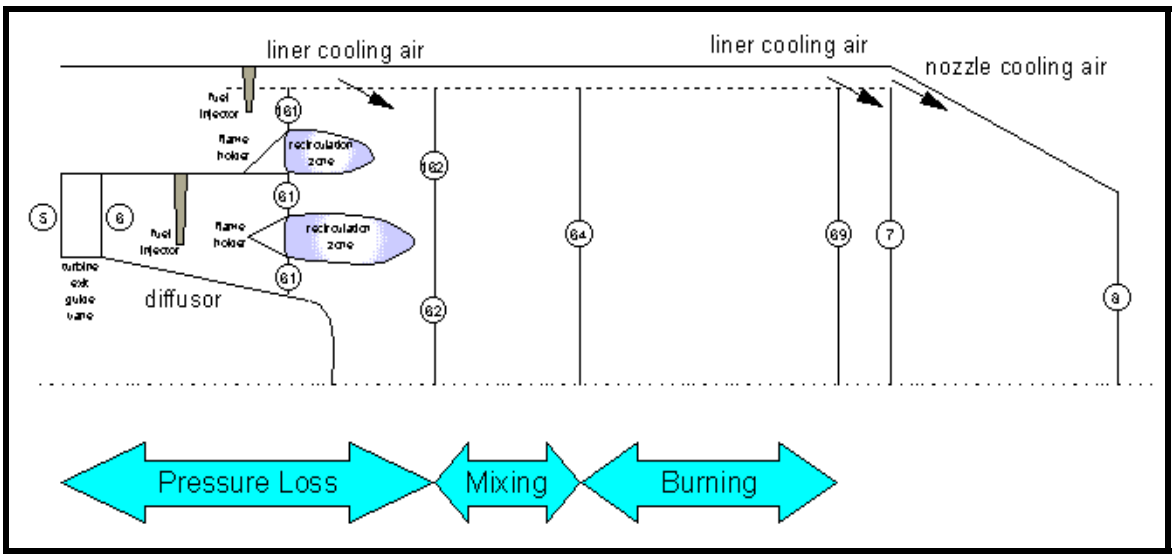

Figure 4.16: Afterburner Nomenclature.

For modeling real engines some empirical corrections to the simple static pressure balance assumption are unavoidable. These are dependent on the details of the afterburner design and no generally applicable advice can be given.

When iterating for an off-design operating point, it may happen that the mixer inlet conditions become quite unrealistic, because the operating points in the turbomachinery maps were estimated badly. The mathematical model of the afterburner must be able to cope with these inlet conditions and calculate the *mixing error* in such a way, that the iteration can converge. In other words, the *mixing error* must change continuously when for any fixed core inlet condition the bypass inlet pressure, temperature, and mass flow change from very low to very high. It must also change, when for fixed bypass inlet conditions the core inlet pressure, temperature and mass flow vary from very low to very high values.

4.2.4.6 Wet (Burning Operation)

4.2.4.6.1 Ideal Temperature Rise

The ideal temperature rise due to combustion of kerosene with air depends on the air inlet temperature, the injected fuel-air-ratio and the pressure in the combustion chamber. Note that the correlation in **Figure 4.17** cannot be applied directly to an afterburner because, at its inlet, the combustion products of the main burner vitiate the air. Nevertheless the figure shows the decreasing return of any additional fuel injection near to the stoichiometric fuel-air-ratio of 0.068.

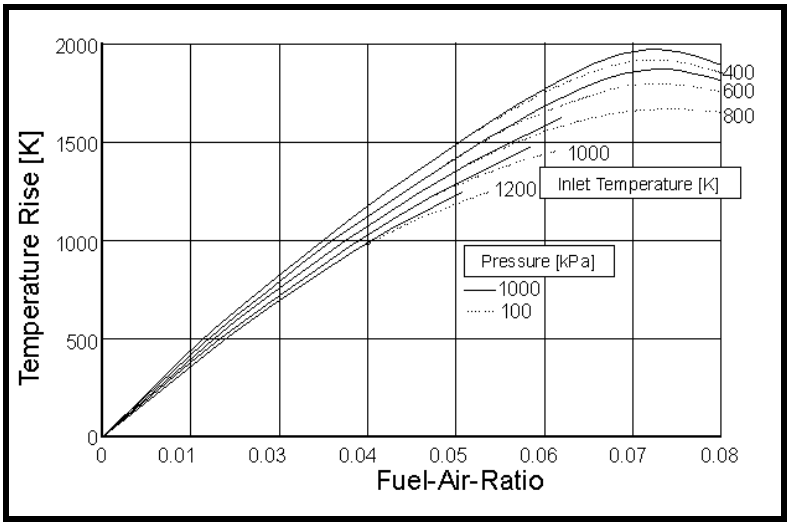

Figure 4.17: Ideal Temperature Rise.

When the fuel-air-ratio is over-stoichiometric, any further fuel addition will decrease the afterburner exit temperature. Keep this in mind, when iterating afterburner fuel flow for a specified nozzle inlet temperature: there are two solutions – or no solution at all when the specified temperature is too high.

4.2.4.6.2 Burning Efficiency

Burning efficiency can be defined as the ratio of achieved temperature rise divided by the ideal temperature rise for a given amount of injected fuel. This definition is good in the normal range of fuel-air-ratios, but leads to peculiar numbers for over-stoichiometric cases.

Alternatively, burning efficiency can be defined as the mass ratio of ideally burning fuel divided by injected fuel. With this definition also the over-stoichiometric regime can be handled consistently. However, the question arises, what happens to the unburned fuel?

Burning efficiency depends primarily on the following parameters:

- Fuel-air-ratio;
- Pressure;
- Inlet temperature; and
- Residence time.

There are complex interactions between these parameters. For example, the fuel droplet diameter and the time needed to evaporate the droplets depends on all four of them. The fuel distribution within the afterburner has also a major effect on the burning efficiency.

Many very different attempts to correlate afterburner efficiency with the parameters mentioned above have been published, however, data required to validate these correlations is not available in the open literature.

4.2.4.6.3 Fuel Injection

The fuel is injected in a staged manner so that the heat addition rate can be increased gradually from min to max. Because ignition, flame stabilization and flame spreading benefit when the fuel-air-ratio is close to stoichiometric, staging is usually produced by adding fuel to successive annular stream tubes so that the mixture ratio in each tube is approximately stoichiometric.

In the core stream of a bypass engine the burning conditions are better than in the bypass stream, and therefore the fuel is injected into the core stream first.

Any fuel injection starts with a liquid. The evaporation of the fuel will cool the main stream and in a precise simulation this effect should be modeled separately, and not regarded as part of the burning efficiency.

4.2.4.6.4 Fundamental Pressure Loss

Adding heat to a flow in a friction-less pipe with constant cross-sectional area causes a loss in total pressure which depends on the inlet Mach number and the temperature ratio T_{69}/T_{64}, see **Figure 4.18**. This pressure loss can be calculated from the laws of mass flow, energy and momentum conservation. When these basic laws are applied to an afterburner, the fuel mass flow must not be forgotten

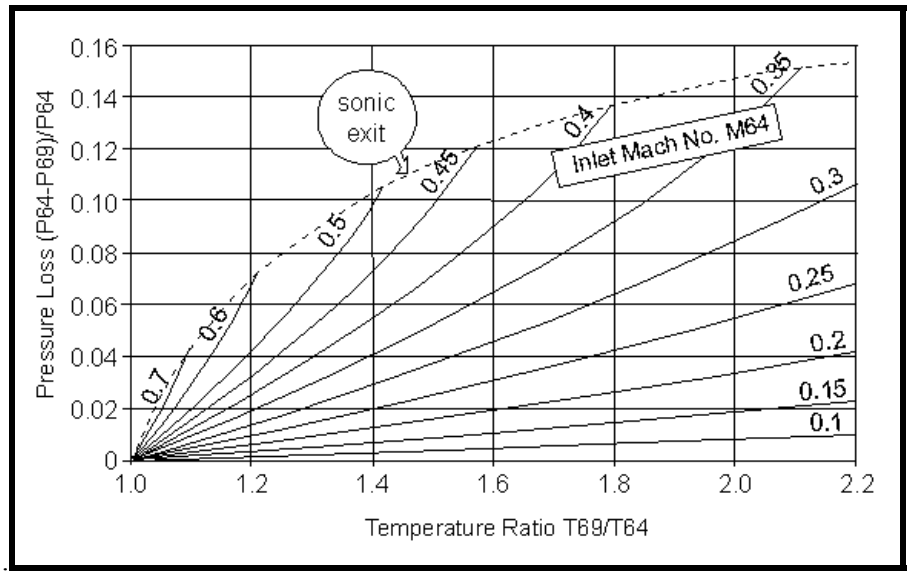

Figure 4.18: Fundamental Pressure Loss.

Some afterburners are not designed with a constant cross-section. In such a case a suitable *effective burning area* must be defined for the calculation of the fundamental pressure loss.

4.2.4.7 Flow Distribution and Cooling

A typical liner requires 8 to 13% of total engine airflow to cool the liner and the nozzle. With a low bypass ratio engine this means, that up to 50% of the bypass air passes behind the liner and does not participate in the burning process.

When the amount of injected fuel is increased from min to max, the afterburner exit Mach number increases, and consequently the static pressure in the jet pipe decreases. The driving pressure ratio of the liner cooling air rises and therefore more of the bypass air passes behind the liner, and less air is left for the burning process.

The nozzle cooling air passes behind the liner and joins the mainstream at the nozzle hinge. When the afterburner is lit, the nozzle cooling air will pick up some heat and therefore the cooling air temperature at the nozzle is higher than at the bypass exit.

The mixing of the liner cooling air with the mainstream is normally modeled neglecting its momentum. The total amount is split in two parts: one part is mixed before, and the rest is mixed after the heat addition calculation.

4.2.4.8 Mixing and Burning

In reality, the mixing of the core with the bypass stream, and the burning process, happen simultaneously. In the simulation, however, these processes are dealt with separately. At first the fully mixed flow conditions at station 64 are calculated. This gives the burner inlet conditions in terms of mass flow, total temperature, total pressure and Mach number. The ideal temperature rise can then be found taking into account the static pressure $P_{s,64}$ and the injected fuel-air-ratio. Remember that some of the oxygen in the air has already been consumed in the core engine combustion chamber.

When the burning efficiency is defined as mass ratio of injected fuel over ideally burning fuel then the true temperature rise is the result of this calculation. Otherwise, the true temperature rise is found as a fraction of the ideal temperature rise.

After the temperature rise calculation the second part of the liner cooling air is mixed to the mainstream and yields the afterburner exit temperature T_7. It is obvious that any number quoted for afterburner efficiency is only meaningful together with a precise description of the liner cooling air model.

4.2.4.9 Test Analysis – Reheat Rig

For the development of afterburners, special rigs are sometimes designed. The supply of bypass air with appropriate temperature and pressure does not pose too much of a problem. However, the core inlet air must be preheated to turbine exit temperature in a burner, and this requires a smaller fuel-air-ratio than exists at the same location in the engine. Consequently there would be more oxygen available than in the engine when no corrective measures are taken (i.e. injection of steam or nitrogen, for example).

In the analysis of a reheat rig test the nozzle inlet mass flow is well known and the total pressure at this location can be derived from static pressure measurements at the end of the liner. The static pressure pickups can be calibrated with the help of CFD calculations, for example. When the effective nozzle throat area is known, one can calculate the nozzle throat temperature and thus the burning efficiency. Note that this test analysis method requires an accurate measurement of the geometric nozzle area, which is very difficult.

When the burning efficiency found from rig tests is applied within total engine simulations, one should be extremely careful. The numbers quoted for the efficiency depend on the liner cooling air model that is used in the rig test analysis.

4.2.4.10 Test Analysis – Gas Sampling

Gas analysis is a tool that gives information about local fuel-air-ratios and local efficiency. The measured values are regularly very high, but they cannot be used for performance simulations because the cooling air is not taken into account. Gas analysis is more a tool for checking the fuel distribution and for optimizing the fuel injection system.

4.2.4.11 Test Analysis – Engine Test

There are two methods to evaluate the afterburner efficiency from measurements taken during an engine test. The first method is the same as already described previously in ***Section 4.2.4.9***. Instead of using the nozzle throat area measurement one can alternatively employ the measured thrust to derive the nozzle inlet temperature. This second method requires a high quality simulation of the nozzle performance, because any deficit in the nozzle model will change the numbers evaluated for the afterburner efficiency and may thus give a wrong impression of the afterburner performance.

However, during dry engine tests the nozzle simulation can be calibrated because then the nozzle inlet temperature is known very well. Therefore, a method that uses the measured thrust, to evaluate the afterburner efficiency, should be preferred. A detailed description of an engine test analysis methodology is given for example in the paper by Kurzke (1998) **[4.3]**.

4.2.4.12 Efficiency Correlations

4.2.4.12.1 One-Stream Models

In a one-stream model the afterburner combustion process begins with the fully mixed flow conditions in station 64 (see **Figure 4.16**). A part of the liner cooling air has already been mixed with the mainstream. Then the temperature increase and the fundamental pressure loss are evaluated between stations 64 and 69. After that follows the mixing of the rest of the liner cooling air.

There is no way to calculate the afterburner efficiency from theoretical considerations with sufficient accuracy. Therefore only empirical correlations, in which the effects of the following influences must be included, can be used:

- Fuel-air-ratio;
- Inlet pressure; and
- Residence time.

For engines with fuel injection into the bypass stream, the fuel evaporation process has an influence on the afterburner efficiency. This can be taken into account by introducing the bypass exit temperature as an additional parameter.

Instead of the residence time, the inlet Mach number is often used in empirical correlations. From a philosophical point of view this is not correct, because the burning process – a chemical reaction – has nothing to do with the Mach number similarity which describes compressibility effects on a flow-field. In practice, however, since the Mach numbers at these locations are generally very low, the Mach number is proportional to the velocity and thus directly connected to the residence time.

At a given flight condition, the afterburner inlet Mach number is also directly connected with the bypass ratio, which varies with the nozzle throat area. Therefore, in empirical correlations for the afterburner efficiency, one can also use the bypass ratio as a parameter that represents the residence time, as shown in **Figure 4.19**.

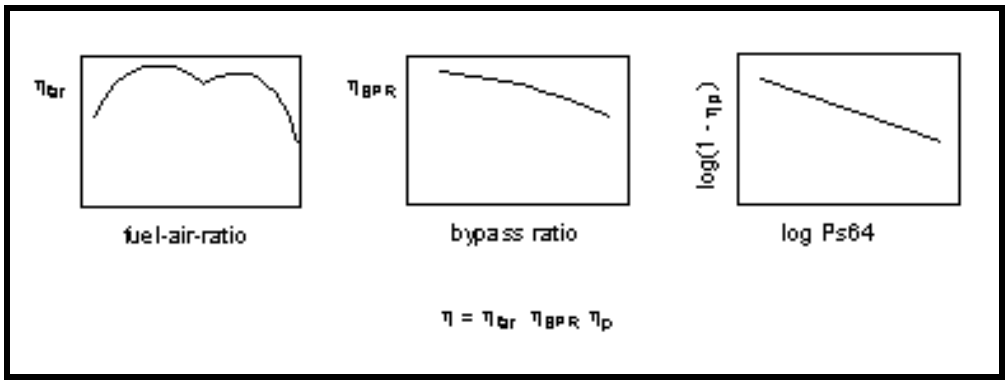

Figure 4.19: Empirical Efficiency Model.

4.2.4.12.2 Multi-Stream Models

The conditions for fuel evaporation in particular, for the core and the bypass stream are quite different. This has led to attempts to set up simulation models that differentiate between the processes in several regions of the afterburner. Such models theoretically have the potential to provide more insight into the system. When they are validated, they could be used for optimizing the fuel staging process, for example.

However, the superiority of multi-stream models over the one-stream model described above has not yet been proven with true test data.

4.2.4.12.3 3-D Codes

There exist several commercial codes, as well as company developed computer codes, for the analysis of combustors. These codes give an insight into the flow distribution and the burning process. However, for engine performance simulations they are far too complex.

4.2.4.13 Blow-Out

Blowout occurs when the rate of heat release in the wake of the flame-holder becomes insufficient to heat the incoming mixture to the required reaction temperature. Important parameters are (local) fuel-air-ratio and velocity. A typical flame-holder stability limit is shown in **Figure 4.20**.

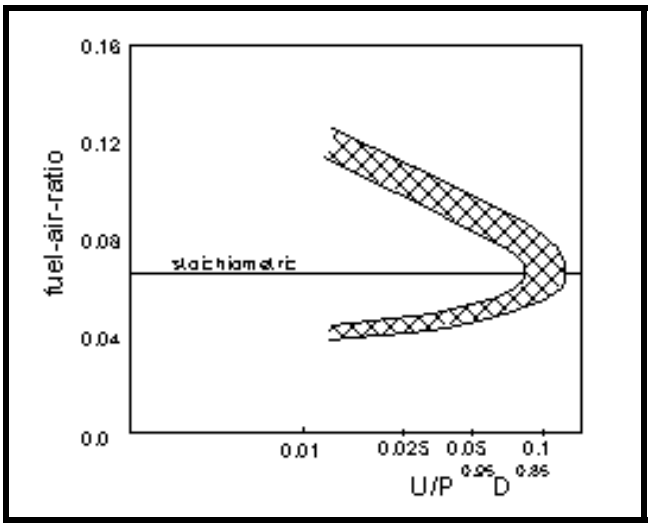

Figure 4.20: Stability Limits.

In the flight regime where the fan stream air flow is cold (i.e. 350 – 400 K) and the pressure is low (50 – 100 kPa), that is, in the upper left hand corner of the flight envelope, fuel vaporization is poor. Hence, uniform gaseous fuel-air mixtures are nonexistent, and two-phase mixtures create ignition and combustion problems that may result in rumble blowouts.

4.2.4.14 Screech

Screech is a high frequency pressure oscillation with 1500 – 3000 Hz in radial direction, caused by variations in the heat release process. It can be very destructive to the hardware and must be avoided under all circumstances. The oscillations can be damped, by incorporating a perforated or corrugated shield in the liner just downstream of the flame-holders.

4.2.4.15 Buzz (Rumble)

Rumble is a low frequency (50 – 100 Hz) pressure oscillation in a longitudinal direction caused by intermittent rich extinction. The explanation given in the paper by Hattingh (1993) [4.5] is that locally the flame goes out and a volume of unburned fuel-air mixture travels down the afterburner, explodes at some point and sends a pressure wave upstream. The pressure wave hits the flame-holder and restores light up, due to the higher pressure restoring local combustibility.

Buzz can be a problem when its frequency is in resonance with a low-pressure spool torque vibration mode.

4.2.5 Inlets

Inlet models generally define the engine model boundary conditions based on both environmental conditions as well as the pressure loss or flow capacity limitations of the inlet device. These models may also address distortion (both pressure and temperature) or other asymmetric boundary conditions due to the inlet or the environment.

4.2.5.1 Inlet Function

The inlet aerodynamic design characteristics of the powerplant have significant effects on the engine performance and stability and are of vital concern to the engine designer. Inlets are designed to guide required engine flow into the front face of the engine with minimum loss and distortion. For sub-sonic flight

velocity this generally means properly faired inlet surfaces to minimize flow separation. For supersonic flight velocity, the design must minimize losses due to formation of shock waves. In any case to assure engine stability, the inlet design must provide low flow distortion and, in the supersonic case, stable shock structures. The inlet design will also have important effects on overall flight vehicle drag.

The inlet functions as follows in the overall powerplant system:

- It accelerates or decelerates ambient air to the engine forward flange station to achieve the entering flow Mach number that will provide most efficient operation of the engine turbomachinery.
- It is part of the cycle compression process.
- It transforms the dynamic pressure generated by flight velocity to increased cycle static pressure.
- It produces total pressure loss in the outer bypass stream.
- It produces total pressure loss in inner core stream by means of spinner scrubbing.
- It affects distortion entering the engine.
- It affects noise generated by powerplant.
- It contains instrumentation required for power setting and engine control.
- It produces 'spillage drag force' due to non-isentropic effects.
- It produces additional air vehicle drag due to scrubbing and pressure forces generated by free stream flow over the external cowl.

Inlet drag and pressure loss should be faithfully modeled in the engine simulation to calculate accurate average total pressures for the core stream and the bypass stream at the fan inlet face. Clear definitions are required for thrust-drag bookkeeping.

4.2.5.2 Inlet Internal Losses: Inlet Recovery

The entering flow stream tube has a stagnation point at the inlet lip. Flow within the stream tube enters the engine and scrubs the inner surface of the inlet creating a boundary layer and reducing the effective total pressure of the flow in the fan tip region. Additional loss due to flow distortion may be generated by inlet lip-separation effects. The flow also scrubs the center spinner producing an additional pressure loss in the core stream. These losses reduce P12 and P2 at the fan or compressor face inlet, and are correlated for simulation as functions of the corrected airflow. This is shown schematically in **Figure 4.21**.

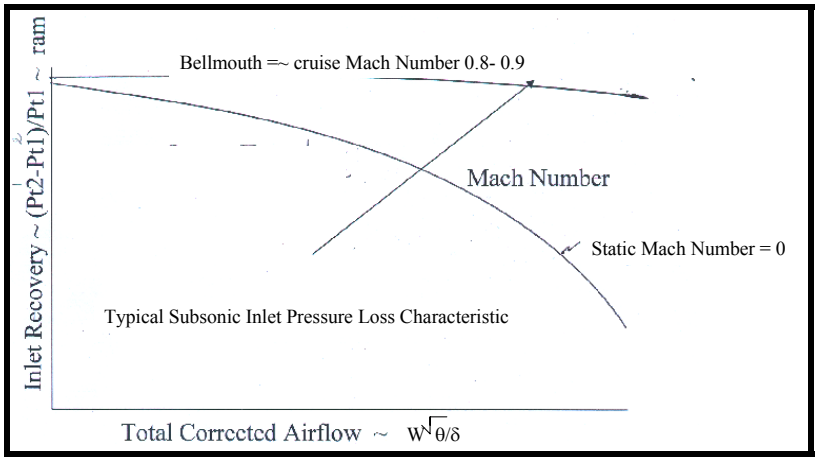

Figure 4.21: Inlet Recovery Loss.

4.2.6 Exhaust Nozzles

The nozzle exhaust system is a major component of an aircraft gas turbine powerplant. It is the device by which the energy from the gas generator is converted into useful thrust. It has efficiency just like other components. Turbofan and turbojet engines are especially sensitive to nozzle losses because they operate on all of the flow from both airflow and thrust standpoint. Careful design to keep losses low is necessary to achieve goal performance.

The exhaust nozzle component system serves the following functions in the aircraft gas turbine powerplant:

- The exhaust nozzle component contains the exit throttling area (throat) of the powerplant. It meters flow and sets the turbine back-pressure, thereby controlling turbine work. It is one of the primary metering areas in the engine, regulating the cycle. For the case of a dual stream bypass engine, the exit nozzle is the principle controller of the back-pressure to the fan thereby setting fan pressure ratio.
- The nozzle functions as an aerodynamic component that accelerates the gas exiting the turbine to produce thrust from available energy -- states 5 – 6 or 5’ – 6’as illustrated in **Figure 4.22**.
- A variable area nozzle plays an important role in providing optimum performance and assuring engine operability. Variable throat area is essential for control of engine matching and fan back-pressure during augmentation.
- A variable geometry nozzle can be designed to generate pitch and yaw forces to control the air vehicle.
- The exhaust nozzle can be designed to produce reverse thrust.

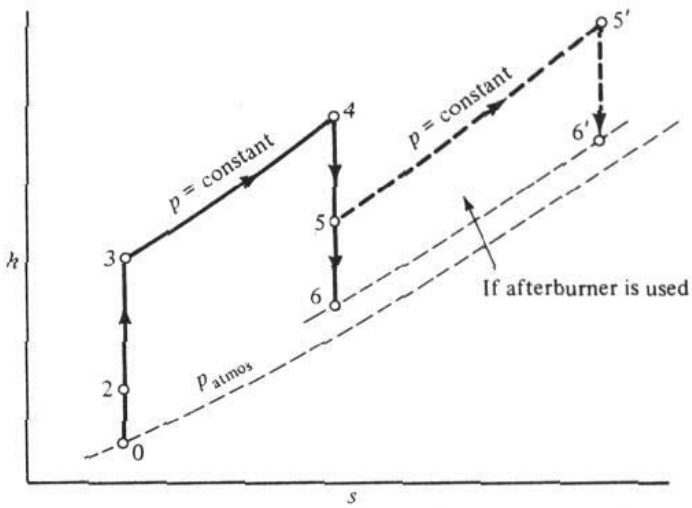

Figure 4.22: Energy Available to Produce Thrust from Thermodynamic Cycle.

The exhaust nozzle is generally represented like other flow restriction devices except for the special relation to thrust calculation and assumptions that can be made concerning choked flow or compatibility condition implied by the expansion to ambient conditions. Most nozzle representations that include detailed thermodynamic properties enforce frozen composition in the supersonic section downstream of the nozzle throat.

When noise is an issue, the nozzle model will generally include additional jet velocity and ejector mixing calculations.

4.2.7 Splitters and Mixers

4.2.7.1 Splitters

Splitter models are often simple bookkeeping models and require no more component-modeling effort than for simple ducts. The flow split will be iterated to match continuity conditions elsewhere in the simulation. An exception is when the splitter model is related to upstream or downstream systems. A common example is the behavior of the splitter downstream of a fan component. Here the flow split or bypass ratio may affect the fan performance via the relative axial location and other geometry details. For models addressing hail or rain ingestion, modeling of the splitter effect on capture of the liquid/solid particles is the primary driver in determining engine operability limits.

4.2.7.2 Mixers

Mixers are employed with high bypass turbofans for thrust increase and for noise reduction. In low bypass engines there is a mixing of two streams within the afterburner. In both cases the flow conditions within the mixer will have a dominating effect on the matching of the two spool speeds of a turbofan.

The thrust improvement due to mixing of two streams ideally – i.e. without friction pressure losses – depends on the difference in total temperature. When both streams have the same total temperature then there will be no thrust gain.

Figure 4.23 shows the ideal thrust gain by mixing two streams with equal total pressure.

When the mixer is applied to a turbofan engine then at cruise the ideal gain in net thrust is typically twice as big as shown in the figure because 1% change in gross thrust is equivalent to 2% in net thrust.

Mixers, like any other component, perform less than ideally in practice. To fully mix two confluent streams needs a long pipe. When forced mixers (chutes) are applied, the required length becomes shorter. In practice, confluent mixers achieve about 20 – 30% mixing and forced mixers approximately 60 – 80%. Moreover, the mixing process and the additional wall friction cause total pressure losses that decrease the benefit of mixing.

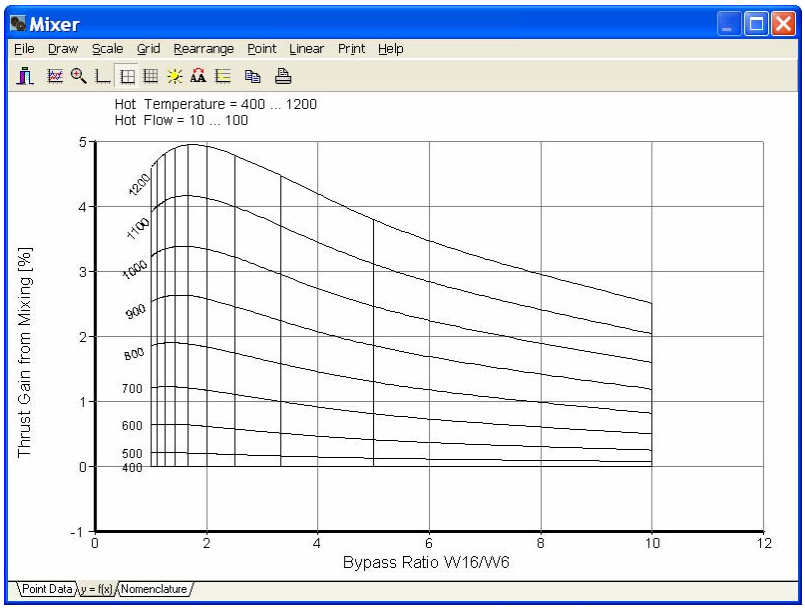

Figure 4.23: Thrust Gain from Ideal Mixing of Two Streams with Equal Total Pressure.

4.2.7.2.1 Definitions

We have spoken of the degree of mixing without defining what we mean with that term. For performance simulations the degree of mixing is defined through thrust:

$$\eta_{mix} = \frac{F_g - F_{g,unmixed}}{F_{g,fullymixed} - F_{g,unmixed}} \qquad \textbf{Eq. 4-19}$$

The evaluation of the thrust for unmixed and ideally mixed streams must be based on a clear definition. **Figure 4.24** shows the nomenclature that we will use here.

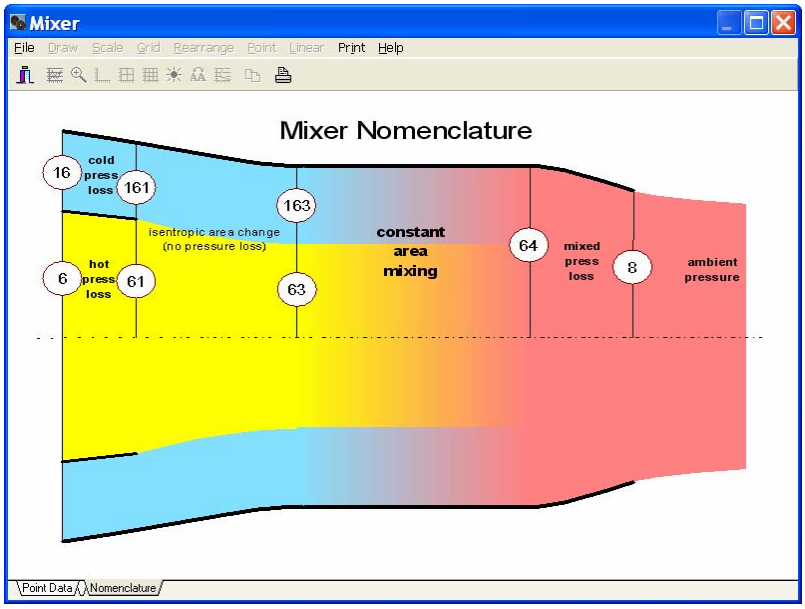

Figure 4.24: Mixer Nomenclature.

The ideal mixer has no pressure losses from stations 6 to 61, 16 to 161 and 64 to 8. At station 64 both streams are fully mixed and expand as a single stream without any losses through the nozzle, which might be convergent or convergent-divergent.

The total pressure and temperature of the cold stream in station 163 are the same as at station 16 and the equivalent is true for the hot stream. The ideal mixing is taking place in a frictionless duct with constant area. The following laws of physics are applied:

***Conservation of Mass*:**

$$W_{63} + W_{163} = W_{64} \qquad \textbf{Eq. 4-20}$$

***Conservation of Energy*:**

$$W_{63} * H_{63} + W_{163} * H_{163} = W_{64} * H_{64} \qquad \textbf{Eq. 4-21}$$

***Conservation of Momentum*:**

$$W_{63} * V_{63} + P_{s,63} * A_{63} + W_{163} * V_{163} + P_{s,163} * A_{163} = W_{64} * V_{64} + P_{s,64} * A_{64} \qquad \textbf{Eq. 4-22}$$

The mixing shall take place in a duct with constant area, which gives us two more correlations:

$$A_{63} + A_{163} = A_{64} \qquad \textbf{Eq. 4-23}$$

$$P_{s,63} = P_{s,163} \qquad \textbf{Eq. 4-24}$$

This system of equations can only be solved by iteration.

When the flow is expanded from the conditions at station 64, through the nozzle, we will get the thrust for the fully mixed flow.

The thrust which could be developed by expanding the hot flow from station 6 through the same type of nozzle is called the *hot* thrust F_h. Similarly the cold stream expanded from station 16 yields the *cold* thrust F_c. The unmixed thrust is the sum of F_h and F_c.

4.2.7.2.2 Pressure Loss

The loss in total pressure, due to mixing without friction pressure loss, is shown in **Figure 4.25** for the same conditions as in **Figure 4.23**. The total pressures of both streams are the same at the inlet to the mixer.

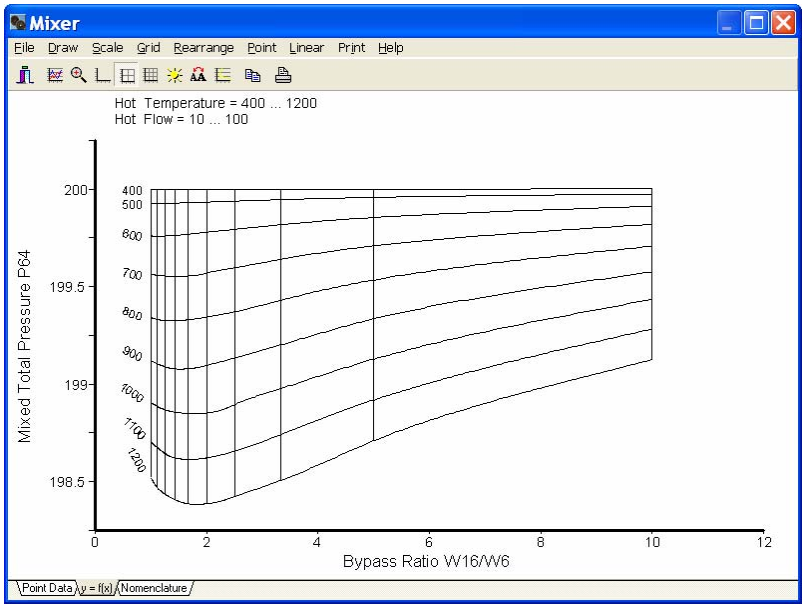

Figure 4.25: Total Pressure after Mixing Two Streams with Equal Pressure (200 kPa).

When the total pressures in both streams are different, then in most cases the pressure at station 64 will be between P_{16} and P_6 and there is no simple way to quantify the pressure losses due to ideal mixing. However, the change in thrust gain due to ideal mixing is a good measure for the influence of the total pressure imbalance at the entrance to the mixer. In **Figure 4.26** we see from an example with $T_{16} = 400$ K and $T_6 = 1200$ K, that any deviation from equal pressures at the inlet will reduce the ideal thrust gain due to mixing.

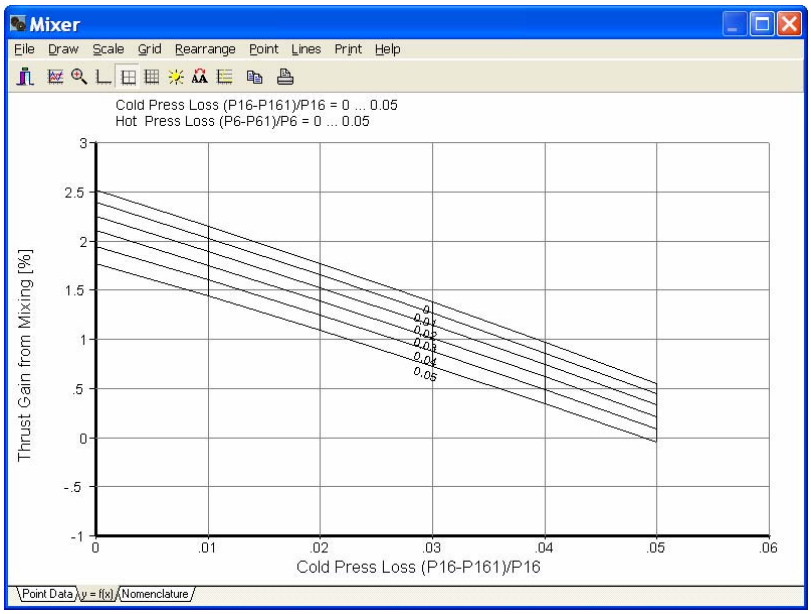

Figure 4.26: Effect of Friction Pressure Losses on the Thrust Gain Due to Mixing.

Unequal total pressures at the inlet to the mixer can cause significant reductions in the thrust gain potential of mixers. Note that in a bypass engine the pressure ratio P_{16}/P_6 will increase when the engine power is reduced. Therefore, the aerodynamic design point of a mixer should normally be at values of P_{16}/P_6 between 0.9 and 0.95.

During all previous discussions we have assumed that there are no friction losses. In reality, these obviously must be taken into account. In **Figure 4.26** (With the assumptions: equal total pressures $P_6 = P_{16} = 200$ kPa at the mixer inlet, $T_{16} = 400$ K and $T_6 = 1200$ K, bypass ratio = 5, mixing efficiency = 70%, $P_{amb} = 101.325$ kPa) the effect of cold and hot friction pressure losses on the thrust gain are shown. It becomes obvious from that figure, that friction pressure losses above approximately 1% in the bypass stream will decrease the benefit of a mixer in such a way, that the weight of the mixer is not justified from a performance point of view. Losses in the hot stream have less effect in this example with bypass ratio 5, because they affect only the smaller mass flow.

4.2.7.2.3 Thrust Gain of Real Mixers

In a practical mixer we will not achieve a fully mixed flow. As mentioned above, in confluent mixers we will get typically 25% and in mixers with chutes roughly 70% of the ideal thrust gain.

We have not yet mentioned the effect of nozzle pressure ratio on the performance potential of a mixer. During cruise with a subsonic high bypass engine, the nozzle flow will be sonic ($P_8/P_{amb} > 1.85$), while during take-off the nozzle pressure ratio will be significantly lower. As can be seen from **Figure 4.27** this will again reduce the potential thrust gain due to mixing.

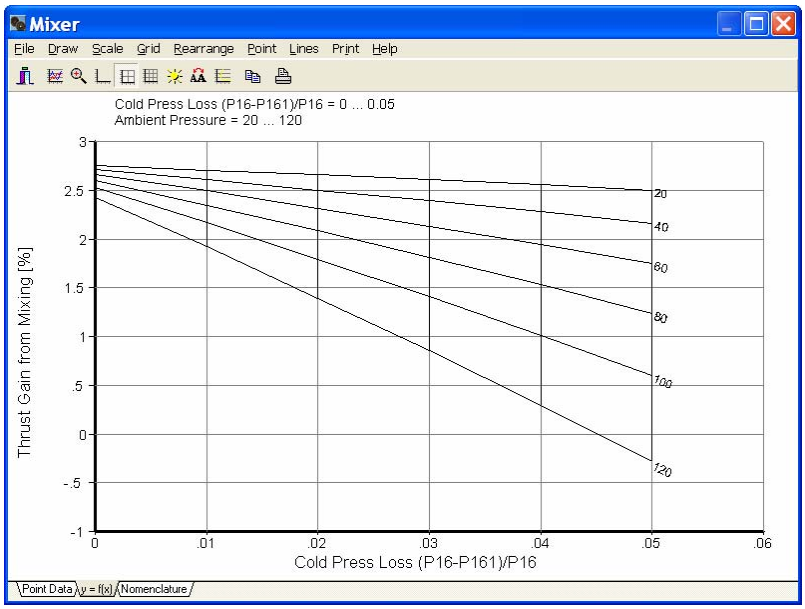

Figure 4.27: Effect of Nozzle Back Pressure on Theoretical Thrust Gain (P8 = 200 kPa).

In a practical mixer with chutes, the real thrust gain due to mixing will be very small for take-off conditions, and typically 1 to 2% during cruise.

4.2.7.2.4 Flow Coefficients

Any flow coefficient is defined as ratio of the area needed for a mass flow at given total pressure, temperature and total-static pressure ratio, and the geometrical area through which this flow passes. Generally, flow coefficients are described by empirical correlations with geometry and total-static pressure ratio.

There are three places in a mixer where flow coefficients must be taken into account. These are the cold and the hot mixer areas A_{161} and A_{61}, and the nozzle area A_8. The upstream conditions for the cold and hot mixer inlet areas are clearly defined and the pressure ratios $P_{161}/P_{s,163}$ and $P_{61}/P_{s,63}$ can be easily evaluated.

The situation for the nozzle is different. The total pressure P_8 at the inlet to the nozzle is only clearly defined when the two streams are fully mixed. For partially mixed flow there is no generally accepted procedure available for the calculation of the mean total pressure at the inlet of the nozzle.

Any formulae that employ the degree of mixing, for the calculation of the nozzle inlet pressure, are not fully satisfactory because the degree of mixing is defined as a thrust ratio. Thrust, however, is dominated (at a given pressure ratio) by the velocity term and thus by the temperature of the fluid, not by the total pressure.

The dilemma with the total pressure downstream of a practical mixer can be bypassed, if the nozzle discharge coefficient is defined in such a way that the ideal flow through the nozzle is calculated from the total pressure of a fully mixed flow.

4.2.7.2.5 Thrust Coefficient

The thrust gain (or loss) due to partially mixing two streams can be described with the help of the *degree of mixing* as defined above. That requires three nozzle thrust calculations: two for the unmixed streams

and one for the fully mixed stream. In each of these nozzle calculations, one applies a coefficient that takes care of nozzle thrust losses, to the one-dimensional calculation result.

In principle, with this approach we use two additive thrust corrections within the calculation.

Alternatively one can use the fully mixed flow as a reference, do the nozzle calculation only once and afterwards apply an empirical correction factor. This is equivalent to the standard procedure for any turbo-machine, where we do an isentropic calculation first, and then apply an efficiency to correct the result. Such an approach eliminates any debates about the nozzle inlet total pressure for partially mixed flow.

4.2.7.2.6 Static Pressure Balance

When two parallel streams are mixed then there will be equal static pressures in both streams. This fact is used within any custom cycle calculation for mixed flow turbofan engines, as a condition for finding the match of the low and high-pressure spool speeds.

In real engines the flow in both streams will not be exactly parallel. However, this is mostly neglected and it is postulated in **Figure 4.23**, for example, that the static pressure P_{s61} equals P_{s161}.

For high bypass engines with corrugated or confluent mixers the simple static pressure balance is fully appropriate. In low bypass engines with afterburner, however, the complex flow in the region of the flame-holders can cause a local static pressure imbalance. The cycle match of such an engine must employ some empirical corrections to the conventional static pressure balance assumption.

4.2.7.2.7 Mixer Test Analysis

The analysis of mixer-component tests is rather difficult because the thrust differences between alternative configurations are rather small. For more details see Rowe, 1982 **[4.6]**. Comparing various mixer designs with the help of engine tests is extremely difficult. The reason is, that there are not only differences in the degree of mixing, but also (at least potentially) in the effective areas at the mixer inlet and the nozzle. These differences will cause the engine to rematch and this in turn will cause a change in fan efficiency, for example. In the end, the engine with the superior mixer design might have a poorer SFC because its effective areas are not correctly matched to the cycle.

4.2.8 Ducts

Most component-based engine models include a large number of identified stations within the engines. Many of these differ only by a pressure loss or a simple extraction of flow that is not explicitly modeled. These pressure loss models are usually modeling a friction loss (Fanno line) process or a loss due to sudden expansion, separation or even an un-modeled low level mixing process. Often these are modeled as an empirical function of velocity head or flow Mach number. Most models are explicit, based only on entrance quantities and thus do not require a compatibility condition closure like nozzles, compressors and similar component models.

If flow in the duct can be choked in any operating regime of interest, this is no longer true. The duct model must address this choking and the simulation must address the implied compatibility condition or the simulation must be configured to address or avoid the issue. For higher fidelity models, the duct model must address the transfer and modification of the more detailed entrance conditions as well as the higher fidelity modeling of the processes inside the duct.

4.2.9 Customer Bleeds and External Loads

Most component-based engine models include the direct effect of bleed between components as a standard feature. For empirical models, the greater the flexibility in bleed level and location, the more tables or

correlations are required to achieve the desired effects. Internal bleed must consider the impact on component performance and the method of determining the conditions of the bleed air. In trying to match bleed supply conditions to user requests, a single bleed location may not be adequate. Bleeds from multiple locations may be selected or mixed to create the required bleed with minimal impact on the overall engine performance.

External load models are generally fixed or simple relationships, and are treated by simply including them as one of the power-outputs from the rotating shaft. For some applications, these models become more complicated and are included as part of the basic engine simulation. This is particularly true where control systems are part of the model and customer load affects the ability to maintain the required conditions.

4.3 NON GAS PATH COMPONENT CHARACTERISTICS REQUIRED BY ENGINE MODELS

4.3.1 Lubrication and Fuel Systems

In models where the fuel and lube system fluid conditions are of interest, these components are modeled similarly to other components except for the use of a non-air working fluid. Most performance simulation applications are not interested in these internal details. In these, fuel and lubrication systems are often empirically modeled as parasitic loads, even in fairly detailed models. In models where conditions in the engine are dramatically affected by these loads, or where the secondary systems interaction are of interest, more detailed models of the pumps and processes in these systems may be required. These models typically include pumping losses (e.g. parasitic losses) modeled as a function of fluid viscosity. Accurate modeling of these losses is particularly important for transient models that are used to predict starting and free windmilling characteristics. This is particularly important for high altitude and cold day operation, where these losses are a larger percentage of output power.

4.3.2 Thermal Management Systems

Military aircraft often have fairly extensive arrangements to reject excess heat from the aircraft and aircraft sub-systems. The engine can be part of this process, and engine models are used in optimizing these systems.

Apart from the turbine, which requires significant attention in terms of managing the cooling flows necessary to maintain component temperature levels, many other parts and systems in a gas turbine engine require management of thermal properties. There are several parts which, without special measures, would get overheated and fail. The major function of the oil system is cooling of bearings; many other parts are cooled by secondary airflows. Fuel often has to be heated to maintain favorable viscous and lubricious properties and to prevent ice formation in the fuel system, or used as a heat sink for excess heat loads. On some classes of aircraft, such as supersonic transports, rising fuel temperature may limit flight duration.

Models of these subsystems interact with the flowpath component models as required to calculate the effect on component performance and to estimate temperatures at key locations.

Separate dedicated models are also used to analyze cooling system performance. These models include heat generation sources in the engine, fuel heaters, oil coolers, fuel-oil heat exchangers and fan air flow models for air coolers. **Figure 4.28** shows a Fokker100/RR Tay engine heat management system model in Simulink. This is used for analysis of cooling performance during engine and aircraft transients. The results were used for preliminary sizing of heat exchanger components.

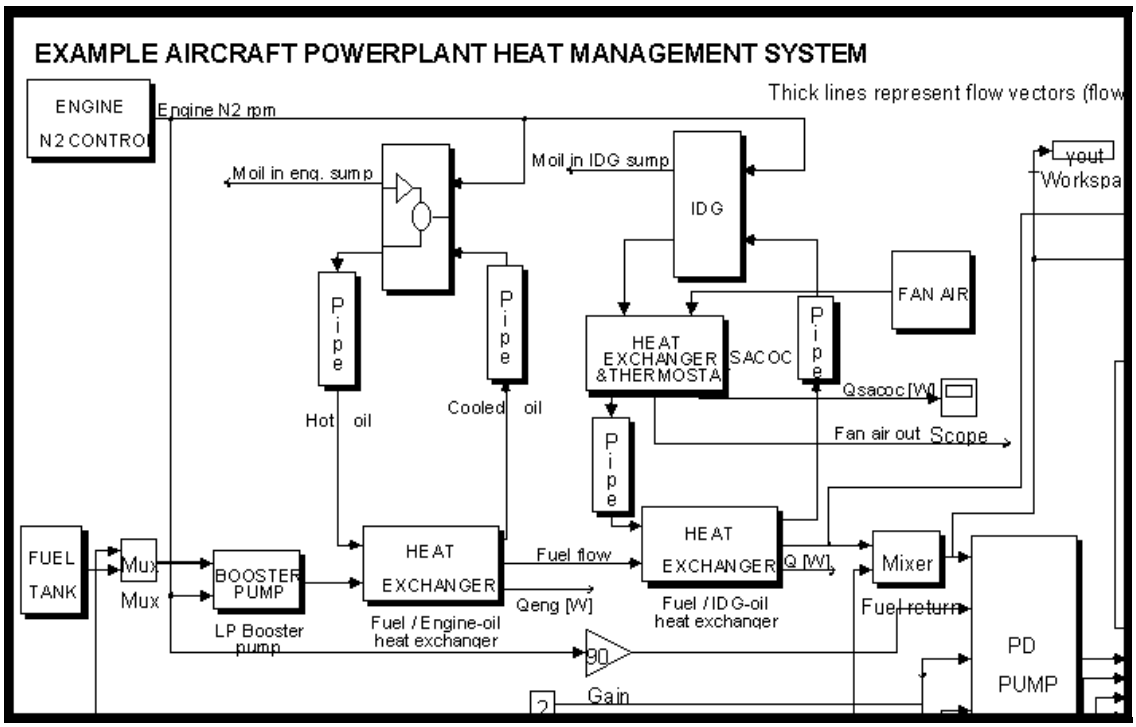

Figure 4.28: Simulink Powerplant Heat Management System Model (top level).

4.3.3 Heat Exchanger

Heat exchanger components in gas turbine cycle models are used to simulate components that are meant to transfer heat into or out of the gas path at some point in the cycle. Most common are heat exchangers such as recuperators or intercoolers.

For a cycle model, primarily overall heat exchanger performance is relevant, including the amount of heat transferred from one medium or heat source to another. Efficiency of the process usually is expressed with "Effectiveness" which is defined as the ratio of actual heat transfer rate Q and the maximum heat transfer that would technically be possible given the media inlet temperatures.

4.3.3.1 Steady State Heat Exchanger Performance

Usually, heat exchangers in gas turbines are of the counter-flow type for maximum effectiveness. The equations for the effectiveness efficiency of a two counter-flow heat exchanger are:

$$Eff = \frac{C_{hot}}{C_{\min}} \cdot \frac{Tt_{in_hot} - Tt_{out_hot}}{Tt_{in_hot} - Tt_{in_cold}} = \frac{C_{cold}}{C_{\min}} \cdot \frac{Tt_{out_cold} - Tt_{in_cold}}{Tt_{in_cold} - Tt_{in_hot}}$$

$$with:$$

$$C_{hot} = Cp_{in_hot} . W_{in_hot} \quad ; \quad C_{cold} = Cp_{in_cold} . W_{in_cold} \qquad \textbf{Eq. 4-25}$$

$$C_{\min} = MIN(C_{hot}, C_{cold}) \; ; \quad C_{\max} = MAX(C_{hot}, C_{cold})$$

$$Rc = \frac{C_{\min}}{C_{\max}}$$

The attraction of using Effectiveness is that if the inlet temperatures and flow rates of both flows are known, the exit temperatures and heat transfer rate can be directly calculated. For a first order approach analysis, with no specific heat exchanger data, a constant effectiveness may be used, representing a typical state-of-the-art value for a particular type of heat exchanger. For detailed analysis, an effectiveness map for a specific heat exchanger may be used. This map usually represents effectiveness as a function of C_{hot} and C_{cold} or W_{hot} and W_{cold}.

After calculating the enthalpies H from the temperatures T at the entry- and exit stations of one of the flows, the heat transfer rate Q can be calculated:

$$Q = W_{cold}.(H_{out_cold}-H_{in_cold}) \qquad \text{where } H = F(Tt, \text{GasComposition}^{1}) \qquad \textbf{Eq. 4-26}$$

In a cycle model, somehow a design point heat transfer rate Q_{des} must be defined. This can be done either by directly specifying Q_{des} or specifying temperature deltas, exit temperatures or effectiveness values. In either case, the design point Q_{des}, Eff_{des} and exit temperatures can all be calculated using:

$$\textit{for counterflow}:$$

$$Q = Eff.C_{min}.(Tt_{in_hot}-Tt_{in_cold})$$

Eq. 4-27

$$so:$$

$$Eff = \frac{Q}{C_{min}.(Tt_{in_hot}-Tt_{in_cold})}$$

Since effectiveness can be expressed as a function of heat exchanger entry temperatures only, off-design heat flux is calculated directly from a given off-design Effectiveness using **Eq. 4-27**. Eff is directly user specified or obtained from a map. An effectiveness map represents Eff depending on the flow 1 and 2 heat capacity rates WCp1 and WCp2.

Depending on the interaction of the heat exchanger with the cycle, the heat exchanger operating point adds equations to the set of equations representing cycle off-design performance. For an intercooler for example, no equations are added since the coolant flow does not directly interfere with the gas path flow. However, for a recuperator, heat is transferred from one point in the gas path back to an upstream point in the gas path, which means that at least one equation is required to satisfy the energy balance in the recuperator. An extra state variable (extra unknown in the set of equations) must be added also, being part of the solution representing a valid operating point found by the solver.

Pressure losses in the flow passages usually are significant. Moreover, for transient performance analysis, with the usually large internal volume and mass of heat exchangers, volume and heat soakage effects are very significant. Therefore, heat exchanger models usually include models for pressure loss, volume and heat soakage effects.

4.3.3.2 Heat Exchanger Transient Simulation

Heat exchangers in the gas path have several specific effects on transient performance. Especially with recuperators, heat soakage effects of the wall between the flows usually are significant and may well cause instabilities during severe accelerations or decelerations without special control system logic. Also volume

[1] This is the more exact version of the approximate calculation of heat flux using constant Cp:

$$Q = W.Cp_{cold}.(Tt_{out_cold}-Tt_{in_cold})$$

effects may be significant if the internal volumes are relatively large. Heat soakage effects of the outside walls usually are small, i.e. similar to other gas path components.

4.3.3.3 Heat Soakage Effect Models

An example of a 0-D heat soakage effect model for the wall between the gas flows is the GSP (NLR Gas turbine Simulation Program, [4.7]) recuperator model. Similar to the external 'insulated wall' heat sink model, the heat exchanger wall heat sink model is based on a first order lag behavior of the average temperature of the material. The difference is that now there are heat fluxes from both sides of the wall and also there is heat flux during steady state (this is not the case with the external insulated wall heat sink model used in other components like turbines and combustors for example).

4.3.3.4 Recuperator Internal Wall Heat Soakage Effect Model

The steady-state temperature of an insulated wall simply is equal to the gas temperature and also is uniform at steady-state. However, the steady-state temperature of the heat exchanger inside wall material is not uniform and normally has a value between the average temperatures of the two media flows. This average steady-state wall material temperature needs to be calculated and fed to a first order lag transfer function to obtain the actual average wall temperature. The actual heat soakage effect is then represented by the net heat flux into or out of the wall material, which is proportional to the rate of change of the average wall temperature.

Consider **Figure 4.29** displaying the temperature patterns in the flows from average flow temperature to the wall temperature.

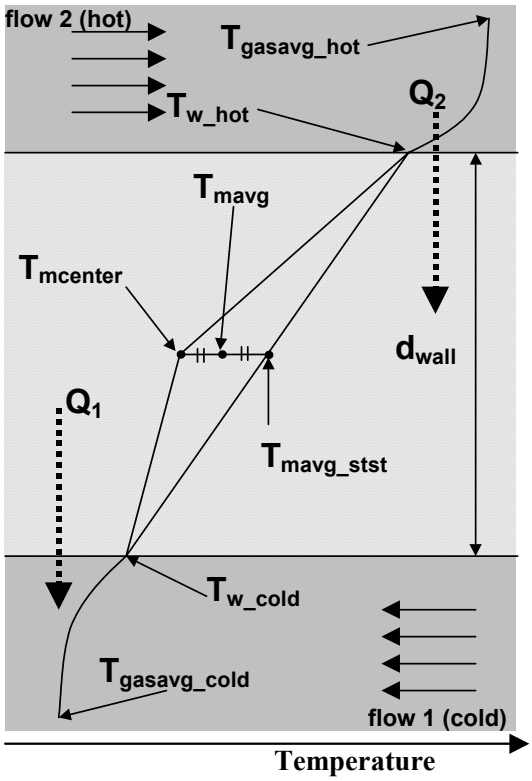

Figure 4.29: Internal Wall Heat Soakage Effect Model.

The temperature pattern in the wall is linear according to the relation for heat flux through a uniform material with conductivity K:

$$Q = A_{eff} \cdot \frac{K_{wall}}{d_{wall}} \cdot (T_{w_hot} - T_{w_cold}) \qquad \textbf{Eq. 4-28}$$

At steady state, Q also needs to satisfy the equations for heat flux from the flows into the wall:

$$Q = A_{eff} \cdot U_{hot} \cdot (T_{gasavg_hot} - T_{w_hot}) = A_{eff} \cdot U_{cold} \cdot (T_{gasavg_cold} - T_{w_cold}) \qquad \textbf{Eq. 4-29}$$

A_{eff} is assumed equal for hot and cold sides. With a uniform wall material specific heat capacity Cp_{wall} and conductivity K_{wall}, during steady state, the average wall material temperature will be equal to T_{mavg_stst}. During a transient, average gas temperatures and flow rates change, and the average temperature level of the wall material will change to a new level, with a certain time lag depending on the total wall material heat capacity and effective area. In view of the high gas flow rates, the effect caused by the heat capacities of the flows themselves is ignored. This assumption may cause some increase in error if one of the flows is completely shut off, resulting in a gradual change in temperature of the medium towards the other flow's inlet temperature. However, for most cases, taking only the wall heat soakage effect into account is considered sufficiently accurate for gas turbines. This assumption also applies to the external wall heat soakage effect (or 'insulated wall') model.

4.3.3.4.1 Steady-State Average Wall Temperature

The average steady-state wall temperature Tmavg_stst is calculated as the average of the wall temperatures Tw_hot and Tw_cold according to **Figure 4.29**. For calculation of Tw_hot, Tw_cold, Tgasavg_hot and Tgasavg_cold, the number of transfer units NTU value is calculated (note that 0 <= Rc <= 1):

$$NTU = \frac{\ln\left(\frac{Eff - 1}{Eff.Rc - 1}\right)}{1 - Rc} \qquad \textbf{Eq. 4-30}$$

$$in\ case\ Rc = 1: \quad NTU = \frac{Eff}{1 - Eff}$$

NTU here represents steady-state heat transfer performance. From NTU, UA can be derived:

$$UA = NTU.C_{min} \qquad \textbf{Eq. 4-31}$$

UA represents the total heat transfer coefficient and the log mean average temperature difference between the two flows then is:

$$dT_{gaslnavgstst} = UA/Qstst \qquad \textbf{Eq. 4-32}$$

From dTgaslnavgstst and the known entry and exit temperatures of the two passages, two temperatures must be determined representing the average gas temperatures at the hot and cold sides of the heat transfer model (Tgasavg_hot and Tgasavg_cold). Note that these are the actual GSP calculated entry and exit temperatures based on the actual heat flux state variables Q1 and Q2, which include the heat soakage effect. This means that Tmavg_stst represents the temperature level that the wall material would obtain for a given Q1 and Q2. In reality however, Q1 and Q2 will change towards a steady-state value Qstst eventually. In effect, an overall heat transfer coefficient UA is used based on steady-state effectiveness

data and this UA is used to calculate the wall temperatures Tw_hot and Tw_cold from the transient heat fluxes Q1 and Q2.

The difference between the average temperatures (Tin-Tout)/2 of both flows is usually close but not exactly equal to dTgaslnavgstst. These must be corrected to exactly obtain dTgaslnavgstst as a difference between Tgasavg_hot and Tgasavg_cold.

Now $U = UA/A_{eff}$ and for the overall specific heat coefficient U also the following relation applies:

$$\frac{1}{U} = \frac{1}{FC_{cold}} \cdot \frac{d_{wall}}{K_{wall}} \cdot \frac{1}{FC_{hot}} \qquad \textbf{Eq. 4-33}$$

The film coefficients FC determine heat transfer between the gas and the wall. For the engine design point a ratio for the two FC is given (default = 1), so with U then the design point FC values can be calculated.

For off-design FC, the following equation is used, derived from a relation for turbulent flow Reynolds numbers obtained from ref. 2 (this equation is the same as that used for the insulated wall heat soakage effect model):

$$\frac{FC}{FC_{des}} = \frac{Cp}{Cp_{des}} \cdot \left(\frac{W}{W_{des}}\right)^{0.8} \qquad \textbf{Eq. 4-34}$$

Now the steady state wall temperatures can be calculated using:

$$T_{w_hot} = T_{gasavg_hot} - \frac{Q_{stst}}{FC_{hot}.A_{eff}}$$
$$T_{w_cold} = T_{gasavg_cold} + \frac{Q_{stst}}{FC_{cold}.A_{eff}} \qquad \textbf{Eq. 4-35}$$

Note that the difference between Tw_hot and Tw_cold is proportional to Qstst according to **Eq. 4-35**.

In case the flow 1 or flow 2 value for FC becomes zero (flow rate zero) the wall temperature is set equal to the temperature of the other flow (the flow medium is entirely assuming the flowing medium's entry temperature and there is no steady state heat flux).

Next the steady state average wall material temperature is calculated:

$$T_{mavg_stst} = \frac{(T_{w_cold} + T_{w_hot})}{2} \qquad \textbf{Eq. 4-36}$$

4.3.3.4.2 Transient Average Wall Temperature

A simplified approximation of the transient wall temperature profile may be represented by $T_{w_hot} - T_{mcenter} - T_{w_cold}$ as indicated in **Figure 4.29**. This 'linearized' profile implies all wall heat capacity is concentrated in the centre and the material between the centre and the wall has no capacity and only conducts heat from wall to centre. It is easy to derive that the actual average wall temperature representing the wall heat content then is calculated using:

$$T_{mavg} = \frac{(T_{mcenter} + T_{mavg_stst})}{2}$$ **Eq. 4-37**

The rate of change in wall heat content dQ is equal to:

$$dQ = h_m.A_{eff}.(T_{w_hot} - T_{mcenter}) + h_m.A_{eff}.(T_{w_cold} - T_{mcenter})$$
$$with:$$ **Eq. 4-38**
$$h_m = \frac{K_{wall}}{(D_{wall}/2)}$$

Eq. 4-38 can be worked into

$$dQ = 4.h_m.A_{eff}.(T_{mavg_stst} - T_{mavg})$$ **Eq. 4-39**

Since dQ in effect is the net heat flux into the material also the following equation applies (with Cp_{wall} and M_{wall} for wall specific heat and mass respectively):

$$dQ = \frac{\partial T_{mavg}}{\partial t}.Cp_{wall}.M_{wall}$$ **Eq. 4-40**

Eq.4-39 and **Eq.4-40** can be combined into the linear differential equation for the average wall material temperature:

$$\frac{\partial T_{mavg}}{\partial t} = \frac{4.h_m.A_{eff}}{Cp_{wall}.M_{wall}}.(T_{mavg_stst} - T_{mavg})$$ **Eq. 4-41**

Eq. 4-41 represents a first order lag system with time constant Tau:

$$Tau = F_{tau}.\frac{Cp_{wall}.M_{wall}}{4.h_m.A_{eff}}$$ **Eq. 4-42**

F_{tau} is a user specified factor with a default value of 1 (see below).

With Tau, now dQ becomes:

$$dQ = \frac{F_{tau}}{Tau}.Cp_{wall}.M_{wall}.(T_{mavg_stst} - T_{mavg})$$ **Eq. 4-43**

T_{mavg} now is calculated by integrating the first order lag system, using a 1st order lag transfer. Using **Eq. 4-37**, then $T_{mcenter}$ can be calculated. $T_{mcenter}$ is a purely theoretical value that is not used in the calculation.

The actual heat fluxes at the cold and hot sides into the material are calculated as follows, by correcting the steady state heat flux Q_{stst}, that is calculated using Eff as described above. Note that Q_{stst} is positive for heat flux from hot to cold flow and Q_1 and Q_2 are positive if adding heat to the gas flow:

$$Q_1 = Q_{hot} = -Q_{stst} - \frac{dQ}{2}$$
$$Q_2 = Q_{cold} = Q_{stst} - \frac{dQ}{2}$$

Eq. 4-44

The deviation dQ/2 of Q_1 and Q_2 from Q_{stst} represent the transient heat soakage effect of the heat exchanger wall. It is assumed the total heat soakage effect heat flux dQ is equally distributed to both flows, which is in accordance to the simplified temperature profile in **Figure 4.29**.

The average heat exchanger wall temperature time constant factor F_{tau} can be changed from the default 1, to adapt the transient heat soakage effect. The value 1 represents the case where all material heat capacity is concentrated in the centre of the wall, which in reality is not the case. The factor may well be decreased to lower values like 0.5, representing a distribution of the heat capacity towards the gas wall boundaries, resulting in faster response of the wall temperature (and smaller heat soakage effects). Also, the presence of fins on the walls can be expressed by lowering the time constant factor (effective area A_{eff} is the effective *plate surface* area excluding fins and should not be adapted for this purpose). Increase of the factor above 1 is not representing a physical meaning and therefore not recommended.

The GSP heat exchanger wall heat sink model is capable of accurately simulating heat exchanger wall heat soakage effects on gas turbine performance. It has limited accuracy in terms of representing the actual heat transfer process as such in detail and should not be used for that purpose.

4.3.4 PowerTrain

Typically, modeling of the power train for steady state operation is done simply by the use of a parasitic load loss function that represents the losses associated with the transfer of mechanical power from the turbine shaft to an external load via a gearbox. In the case of a lubricated gearbox, the losses may be modeled as a function of the viscosity of the lubricating fluid. For transient operation, modeling of these losses become increasingly complex as the losses may be a function of operating shaft speed. An added complexion for modeling of transient performance is the incorporation of a clutch model. This is of interest for such events as engine starting.

4.3.4.1 Clutch Models

A clutch is an unusual element in a gas turbine drive train system. However, there are a number of applications, where the load needs to be coupled and uncoupled from a gas turbine drive shaft during operation. In these cases, a clutch is required to allow smooth transition from the uncoupled state to the fully coupled state and vice versa, without excessive torque loads on the shafts due to high acceleration rates.

Examples of clutches in gas turbine drive trains may be found in vehicular turboshaft engines, helicopter drive trains and STOVL propulsion systems using liftfans driven by the main engine LP shaft.

In general, a clutch is a device that is able to transfer a certain (limited) amount of torque between two shafts. Several systems exist to transfer the torque including wet and dry friction plate systems and a variety of hydraulic systems (e.g. torque converters, hydro-motors). For analysis of system performance, the clutch model minimally needs to accurately represent the torque transferred. If clutch performance also itself requires scrutiny, more detailed models may well be required. This section describes the clutch model as implemented in GSP, [4.7], with calculation of torque transmission, clutch state and friction heat production.

For the clutch model, a number of terms/parameters are introduced to determine the state of operation of the clutch.

- **Engagement Status:**

  A clutch can be fully engaged or disengaged. If fully engaged, it is able to transfer maximum torque capacity; if fully disengaged, usually no torque is transferred unless some sort of residual friction loss is defined in the model. An 'engagement variable' (or engagement factor) is used, ranging from 0 to 1. 0 is fully disengaged, 1 means fully engaged.

- **Locked/Unlocked Status:**

  If a clutch is locked, both shafts run at the same rotor speeds and the clutch functions as a coupling. In this case, the torque transferred does not exceed maximum static torque capacity. If the clutch is unlocked, both shafts are not running equal speeds. There is a case where the clutch is unlocked at equal speeds, but this only can occur during a very short time of transition between the locked and unlocked states, or when at least one shaft is accelerating 'past' the other shaft speed.

- **Static Torque Capacity:**

  Static torque capacity is the maximum torque the clutch can transmit in the locked state. This means the friction surfaces do not move (relative to each other) and the static friction coefficient applies. Static torque capacity always is equal to or larger than dynamic torque capacity.

- **Dynamic Torque Capacity:**

  Dynamic torque capacity is the maximum torque the clutch can transmit when it is unlocked, i.e. rotor speeds are not equal and the friction surfaces are moving relative to each other, so the dynamic friction coefficient applies. Dynamic torque capacity always is equal or smaller than static torque capacity.

- **Torque Demand:**

  Torque demand is the torque that would be transmitted in the locked state. It can also be described as the torque that would exist in the shaft if maximum torque would be infinite and no slipping would occur.

- **Slipping:**

  The clutch is slipping if the two rotor speeds are unequal and engagement is larger than 0. Torque required exceeds maximum dynamic torque capacity and therefore cannot fully be transmitted. This means friction heat is produced proportional to the torque (engagement x maximum dynamic torque) and the delta in rotor speeds.

The operation mode of interest with a clutch model is transient. For steady-state simulation, either the fully engaged or disengaged state must be assumed. For system modeling environments, this means that the reference (usually design) point state also either is fully engaged or disengaged. Prior to a transient simulation, then a fully engaged or disengaged state must exist.

For a particular clutch, a static and dynamic maximum torque must be specified. The engagement factor $F_{engagement}$, ranging from 0 at disengagement to 1 at full engagement, determines the actual torque capacity as a fraction of maximum torque.

The engagement factor during a transient simulation can either be obtained from user-specified time functions or result from a control system model output. With a clutch control model, accurate simulation of clutch performance in complex systems, including closed loop controlled engagement, can be performed.

Friction heat production due to clutch slipping is calculated, and with more data an accurate heat flow and conduction model can be added to analyze local heat loads and temperature levels during and after successive engagement events.

One of the challenges in modeling clutch engagement or disengagement transients is to determine whether static or dynamic maximum torque is applicable. In other words: is the clutch in a locked state or is it slipping. In the transient simulation this means the model algorithm needs to keep track of the clutch state (locked or not) history during transient simulation, i.e. save the clutch state of the prior time step. The state of the prior time step then determines whether dynamic or static maximum torque applies. For example, during a transient starting with a locked clutch but increasing torque demand, at some point this torque will exceed maximum static torque and the clutch will unlock and start slipping.

After the time step where the unlocking has been determined, the lower level of dynamic maximum torque applies, and the clutch can only lock again after the torque demand will drop below dynamic maximum torque. If torque demand fluctuates around maximum static torque levels, severe transient load effects on the clutch can be simulated. In this case however, small time steps will be required to accurately represent rapid transient effects.

In **Figure 4.30** the flow chart for the basic elements of the algorithm is shown. Starting at particular state at time t, actual static and dynamic torque depending on maximum torque capacities and the engagement factor are determined and also the rotor speed delta dN (difference in rotor speeds) is determined.

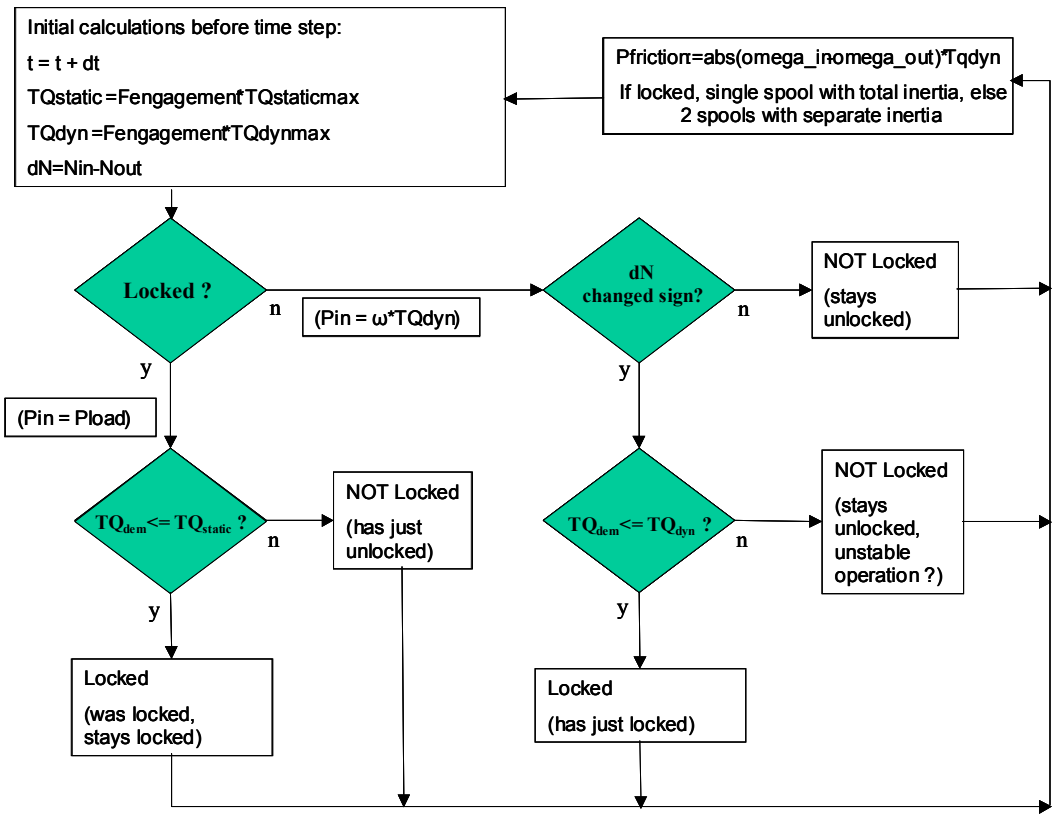

Figure 4.30: Clutch Model Algorithm.

Next the algorithm continues evaluating the Locked state at the prior time step ("Locked ?" decision box) and then determines the new Locked state of the current time step depending on dN and the demanded

torque TQdem. There is a special case (where unstable operation may be suspected) and that is when the clutch was not Locked, dN changes sign (so the rotor speeds have been equal at some point during the last time step but locking could not be established due to excessive torque demand).

After the locked state of the new time step is determined, friction power Pfriction can be calculated and also the distribution of inertia over the shafts can be determined. These inertia values are used when integrating rotor acceleration (at every time step) of either 2 separate shafts (unlocked) or a single shaft with the sum of 2 inertias (locked state). Furthermore, depending on the detail of the model more additional clutch data can be calculated.

In GSP, [4.7] an example is given of simulation of a turbofan driving a STOVL lift-fan through a clutch. The lift-fan is driven by the main engine fan shaft through a dry clutch that is able to disengage the Lift Fan from the engine during normal forward flight and engage during vertical flight modes.

Figure 4.31 shows clutch parameter responses versus time for lift-fan engagement (starting at 0.2 s) and disengagement (starting at 2 s) at 100% main engine N1. The top graph shows clutch engagement in terms of (dynamic friction) torque capacity. Next actual torque delivered to the lift-fan and the heat dissipation (Pfriction) during clutch slipping are shown.

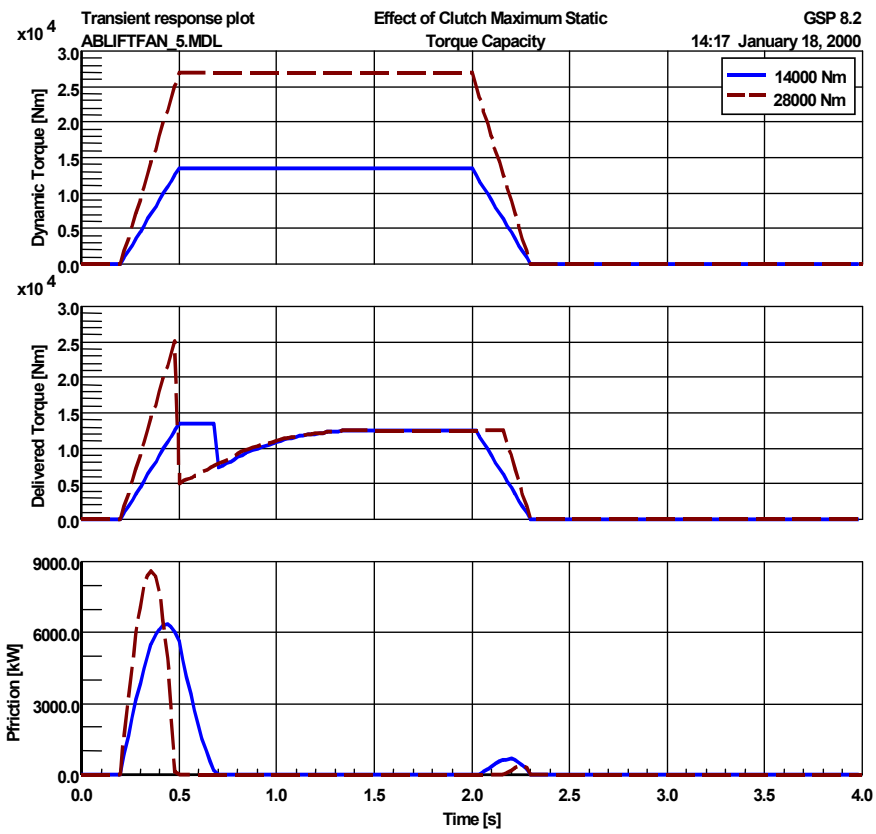

Figure 4.31: Lift-Fan (Dis)Engagement Clutch Response.

Figure 4.32 shows the rotational speeds of the lift-fan and the engine fan in a single graph, effectively summarizing rotor speed and clutch performance histories.

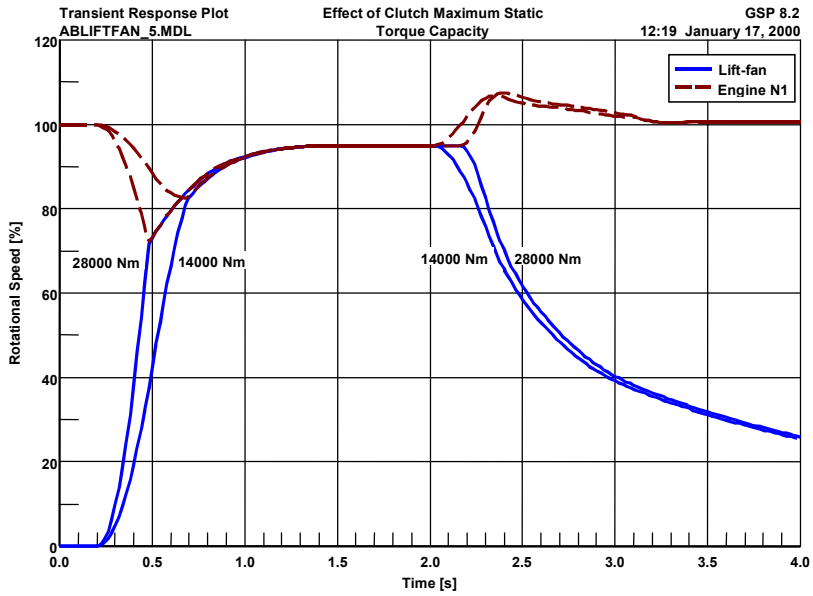

Figure 4.32: Lift-Fan (Dis)Engagement Lift-Fan and N1 Response.

4.3.4.2 Loads

There are many different types of loads, depending on the gas turbine application. For example:

- Generator for electrical power generation;
- Accessory gearbox; and
- Main transmission gearbox and rotary wing (helicopter) applications.

Accessory gearboxes drive such components as cooling fans, pumps and starter motors.

There are different levels of fidelity that can be used to model loads; from a simple constant power extraction to a more complex map for a cooling fan helicopter rotor. These models are usually provided by the load device manufacturer. They convert load demand (e.g. electrical power, mechanical power) into resisting torque or power extraction that applies to the gas turbine cycle.

Typically, load demand requirements that the gas turbine supplies for the customer's specific application change with engine power output.

Mission profiles are defined that provide typical engine power output requirements as a function of operational environment and operating mode (i.e. output power level). Mission profiles enable that analysis of:

- Life duration estimates for critical engine components; and
- Calculate tip clearance excursions for turbine and compressor and verify adequate margins throughout the flight regime.

Transient analysis must be performed in the event of a load shed event. The most severe of which would be due to a break of the power shaft. Transient simulations are used to design control systems to prevent rotor speed excursions that could damage gas turbine hardware. In cases of electrical power faults, inertia of the generator is still present so the overspeed threat is less.

4.4 REFERENCES

[4.1] Society of Automotive Engineers Aerospace Standard AS755 Rev C, Aircraft Propulsion System Performance Station Designation and Nomenclature, December 1997.

[4.2] Recommended Practices for the Assessment of the Effects of Atmospheric Water Ingestion on the Performance and Operability of Gas Turbine Engines, AGARD AR-332, 1995.

[4.3] Kurzke, J. and Riegler, C., "A Mixed Flow Turbofan Afterburner Simulation for the Definition of Reheat Fuel Control Laws", RTO Symposium on Design Principles and Methods for Aircraft Gas Turbine Engines, Toulouse 1998.

[4.4] Egan, W.J. and Shadowen, J.H., "Design and Verification of a Turbofan Swirl Augmentor", AIAA 78-1040, 1978.

[4.5] Hattingh, H.V. et al., "The Design and Development of an Afterburner", ISABE 93-7041, 1993.

[4.6] Rowe, R.K. and Kuchar, A.P., "Energy Efficient Engine, Scaled Mixer Performance Report", General Electric Company, NASA CR-167947, 1982.

[4.7] Visser, W.P.J. and Broomhead, M.J., "GSP, A Generic Object-Oriented Gas Turbine Simulation Environment", ASME Paper # 2000-GT-2, May 2000.